HYDROLYSIS-DRIVEN BUOYANCY PROPULSION SYSTEM FOR SUBMERSIBLES

By: Jo Borchsenius

[18.02.2011]

Primary supervisor: Shane D. Pinder

School of Engineering, Auckland University of Technology

A thesis/dissertation submitted to Auckland University of Technology in partial fulfilment of the requirements for the degree of Master of Engineering

ABSTRACT

The research presented herein intends to improve the flexibility of underwater gliders with the development of a novel propulsion system. The proposed Chemical Buoyancy Drive is indicated to yield up to 20 times the amount of available electric energy and exhibit 90% propulsion efficiency, compared to that of the commercial underwater glider named "Spray" developed by Scripps Institution of Oceanography at a depth of 1,500 m. Its performance is readily optimised to any depth, and there is no need for a thermal incline in the operational environment. Also the need to isolate the energy storage from external pressure is eliminated by the use of lithium hydride suspended in a slurry, which is reacted with seawater to generate hydrogen. The subsequent increase in volume results in propulsion through the induced hydrodynamic forces on the hull and wings, and the hydrogen can be consumed in a fuel cell providing electric energy. A prediction of the drive's performance up to 10,000 m depth is presented, which has been based on data from the studied literature. This has been verified through the developed experiments up to an equivalent of 3,000 m. Additionally, a study on potential improvements and the practical realisation of the system is presented. The proposed Chemical Buoyancy Drive could be a competitive alternative to the propulsion of underwater gliders and other autonomous underwater vehicles.

TABLE OF CONTENTS

LIST OF FIGURES

LIST OF TABLES

LIST OF EQUATIONS

DEFINITION OF PRESSURE ANNOTATION

Gauge pressure [Barg] is defined as the pressure differential to the actual surrounding atmospheric pressure. In this thesis also [Bar] refers to gauge pressure, but here the reference is standard atmospheric pressure equivalent to 760mm Hg. Absolute pressure is annotated as [Bara].

LIST OF ABBREVIATIONS

General:

ALACE	-	Autonomous Lagrangian Circulation Explorer
AUT	-	Auckland University of Technology
AUV	-	Autonomous Underwater Vehicle
CBD	-	Chemical Buoyancy Drive
CTD	-	Conductivity, Temperature, Depth
DOE	-	US Department of Energy
GPS	-	Global Positioning System
HPLC	-	High Pressure Liquid Chromatography
NIST	-	National Institute of Standards and Technology
PEMFC	-	Proton Exchange Membrane Fuel Cell
RAFOS	-	SOFAR spelled backwords
SOFAR	-	Sound Fixing And Ranging
STP	-	Standard Temperature and Pressure
WHOI	-	Woods Hole Oceanographic Institute

Chemical:

$Al(BH_4)_3$	-	Aluminium borohydride
$Ca(BH_4)_2$	-	Calcium borohydride
H_2	-	Hydrogen
H_2O	-	Water
HCl	-	Hydrochloric acid
$LiAlH_4$	-	Lithium aluminium hydride
$LiBH_4$	-	Lithium borohydride
LiH	-	Lithium hydride
$LiOH$	-	Lithium hydroxide
$Mg[BH_4]_2$	-	Magnesium Borohydride
MgH_2	-	Magnesium hydride
$Na3AlH6$	-	Sodium aluminium hydride
$NaCl$	-	Sodium chloride

ATTESTATION OF AUTHORSHIP

"I hereby declare that this submission is my own work and that, to the best of my knowledge and belief, it contains no material previously published or written by another person (except where explicitly defined in the acknowledgements), nor material which to a substantial extent has been submitted for the award of any other degree or diploma of a university or other institution of higher learning."

Signature:.. Date and place: ...16.06.2011....OSLO, NORWAY

Jo Borchsenius

ACKNOWLEDGEMENTS

I hereby extend my deep felt gratitude to Dr. Shane D. Pinder who has been my primary supervisor and provided great guidance and support through the course of this degree.

♦

Equally, I would like to thank Dr. John Robertson. Although he has not officially been my supervisor, he has provided extensive support and guidance in this research in terms of chemistry, as well as in general matters.

♦

Additionally I would like to thank Bauke Blok at Swagelok New Zealand for extraordinary support, Dr. Claude Aguergaray for valuable discussions and encouragement, and Tor Erik Kristensen for his input.

♦

I also appreciate the help I received from Brett Holden, Christopher Yearsley, Percy Perera, Christopher Whyburd, Yan Wang and the other employees at AUT who have contributed to the quality and completion of this work.

♦

Further, I gratefully acknowledge the support from the Office of Naval Research Global, which enabled me to attend the IEEE OCEANS 10 student poster competition in Sydney.

♦

Finally, I extend much gratitude to my friends, colleagues, girlfriend, and family who have all stood by me in the ups and downs of this work, and inspired me to achieve my goals.

1 INTRODUCTION

1.1 SUBJECT OF AND REASON FOR THIS RESEARCH

The research presented in this thesis concerns the development of a novel propulsion system for underwater gliders based on the hydrolysis reaction of lithium hydride and seawater. It is believed that the propulsion systems currently in operation have certain limitations that can be addressed with the proposed concept.

1.2 BACKGROUND TO INVESTIGATION

Through the studied literature it became apparent that the current propulsion systems were a continued development of the existing buoyancy drives used in buoyancy floats. Since the operational objectives of an underwater glider exceed that of a buoyancy float, also the buoyancy drive propelling it can have extended requirements. These requirements can be large variations in operational depths within the same mission, and the need for a more energy intensive payload.

1.3 OBJECTIVES OF THIS RESEARCH

The objectives of the research presented in this thesis are therefore to:

- Predict the performance of the proposed system
- Verify this prediction through experimental testing
- Investigate any conceptual limitations or practical challenges that may arise from the performed experiments
- Compare the performance of the proposed system to that of the existing designs

1.4   LIMITATIONS AND SCOPE OF INVESTIGATION

Although developing the proposed propulsion system and performing subsequent sea trials would have proven the concept, it would have been difficult to accurately determine its optimal performance. Moreover, the cost of extensive trial and error exceeds the budget of this project. Consequently, an accurate theoretical prediction of the performance of the proposed buoyancy drive has been developed, and it has been verified through experimental testing.

1.5   PLAN OF DEVELOPMENT

The thesis begins with an introduction to underwater gliders, and the identified limitations that led to the development of the proposed Chemical Buoyancy Drive. The shortages in the studied literature are accounted for, and the methods used to investigate these are presented. Then, the results from this investigation are presented, giving a practical understanding of the chemical reaction being explored. The results also show the expected performance of the proposed system, and act as verification to the presented theoretical prediction. This is followed by an interpretation of these results, which leads to the drawn conclusions. Finally, recommendations for the continued development are presented.

2   LITERATURE REVIEW

This thesis covers the development of a novel propulsion system for underwater gliders. To understand the limitations of the existing propulsion systems, an understanding of underwater gliders, their design, and their applications is crucial. Consequently, an introduction to these topics is presented in this chapter, followed by a theoretical background and description of the proposed Chemical Buoyancy Drive. Finally, the physical aspects relevant to the system and the shortages in available literature are discussed. The chapter below is intended to give an introduction and a basic understanding of how and why the underwater gliders were developed.

2.1   AN INTRODUCTION TO UNDERWATER GLIDERS

Underwater gliders are a class of Autonomous Underwater Vehicle (AUV) propelled by a change in buoyancy. This change in buoyancy is converted into forward movement by hydrodynamic forces working on the hull and wings of the underwater glider much like a gliding airplane [1]. How the buoyancy change is currently achieved is covered in 2.3. The extended range of underwater gliders sets them apart from other classes of autonomous underwater vehicles. However, this is not because buoyancy propulsion is more efficient than propellers as such, but mainly due to the slow operating speeds that are practically obtainable [1, 2]. The hydrodynamic loss called "drag" has an approximate quadratic relation to operating speed, thus halving the operating speed will reduce the consumption of energy by approximately a factor of 4, which in turn will increase the range [1]. Moreover, the naturally occurring vertical saw tooth pattern of its course through the water accommodates the ocean profiling, which is the underwater glider's primary application [1, 2]. The applications will be covered in further detail in 2.1.3.

2.1.1 HISTORY

The invention of underwater gliders has been a gradual development through the latter half of the 20th century. The invention of SOFAR (Sound Fixing And Ranging) by Dr. M. Ewing in 1948 solved the challenge of underwater localisation by using sound waves. This paved way for the first sub-surface ocean current measurement floats in 1955 [3, 4]. The first floats were neutrally buoyant at a specific depth, but they adopted more functionality through several designs. One such design was the SOFAR float in 1970 that also used the SOFAR system [5]. In 1986, a float was developed that used the inverse of the SOFAR system. It functioned as a receiver instead of a transmitter of the sound signals, and it was named RAFOS, which is SOFAR spelled backwards [5]. In 1991, the first autonomous float ALACE (Autonomous Lagrangian Circulation Explorer) was developed [6]. This was capable of repeatedly resurfacing by using a battery-powered hydraulic system to change its volume and, as a result, its buoyancy. At the surface it was able to communicate position and gathered data through System Argos satellites. In functionality, this float was virtually identical to the first underwater gliders being tested at about the same time, with the exception of wings and the glide path controls found in the underwater gliders [7].

These floats were the basis for the discussions at Woods Hole Oceanographic Institute (WHOI) that led to the development of the first underwater gliders. Since this initial development took place as a result of a discussion, it is difficult to determine who can be credited with the invention. The invention has previously been incorrectly attributed to Henry Stommel [8, 9], due to his much referenced paper; "The Slocum Mission", published in Oceanography in April 1989 [10]. Stommel has been a visionary in the field from the beginning [3] and he has been involved in the discussions that took place at WHOI in 1978 [8, 11]. Nevertheless, it is indicated that Doug Webb, later the founder of Webb Research Corporation (WRC), was a central character in the development of horizontal propulsion to profiling floats [5, 12]. More than a decade passed before these ideas were realised and field tested in 1991 [7]. These tests were led by Paul J. Simonetti, also affiliated with WHOI, and the underwater glider presented in [7] is very similar in concept to the battery-powered underwater gliders of today [1].

Based on how the underwater gliders have been developed, it can be argued that they are buoyancy floats with an active positioning system, rather than being a completely new class of AUVs. Most of the currently operational underwater gliders are an evolution of earlier buoyancy floats and share very similar methods of changing the volume[1].

2.1.2 FUNCTIONALITY

Although there are different designs of underwater gliders, the fundamental functionality stays the same. The size is commonly about 2 m long, weighing about 50 kg and displacing about 50 l of water. As an example of a typical design, an illustration of the commercial underwater glider Spray is shown below.
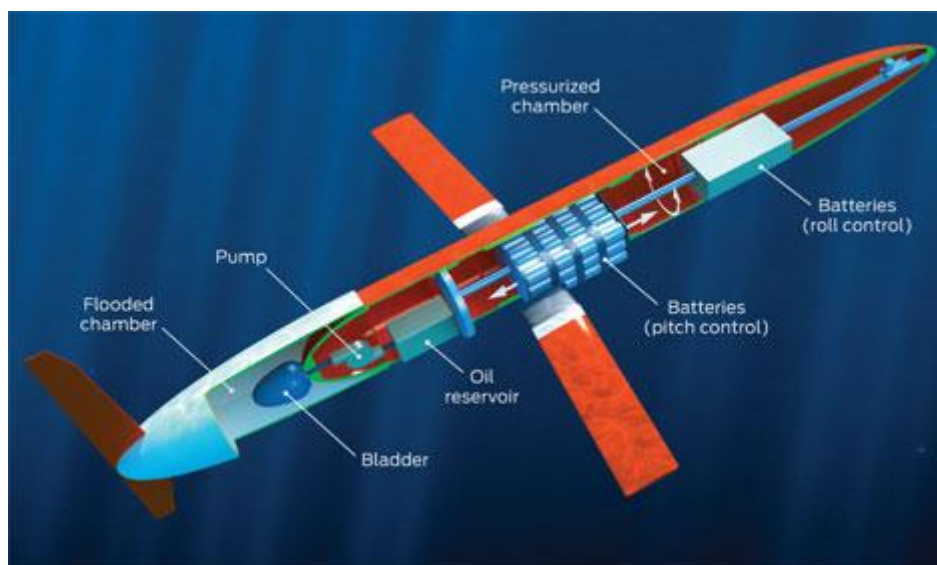
FIGURE 1: ILLUSTRATION OF THE UNDERWATER GLIDER SPRAY [13]

Figure 1 shows the major internal parts of a battery powered underwater glider. The wings and hull convert the buoyancy change achieved using a buoyancy engine, or buoyancy drive, into forward motion through hydrodynamic forces. This hull is controlling the heading by an on board sensor package and control system typically able to adjust pitch and roll by the use of an internally moving mass and external rudders or flaps. While gliding from surface to bottom to surface again the

underwater glider measures specific parameters of the surrounding water using a scientific payload designed specifically for its mission. While at the surface, these results are communicated through satellite communication to a recipient. Since this is a two way communication it is possible to alter the mission objectives for the next dive, or it can be left to continue on its predetermined path without intervention. Additionally, the position is calibrated by GPS at surface, before diving again navigating by recorded direction from the reference at surface. This method of navigation is called dead reckoning and commonly makes use of a compass, depth gauge, and even measured inertia in larger vehicles. This cycle is repeated and the underwater glider travels in a vertical saw tooth pattern with a horizontal speed of typically 0.25 m/s and a glide angle of about 20 degrees to achieve optimal efficiency, but this can vary depending on mission objectives. This glide angle, while advantageous for effective horizontal movement, can be considered vertical when compared to changes in ocean parameters over distance. This gives the equivalent of a vertical profile of the ocean. Travelling in this manner enables underwater gliders to roam the oceans with an impressive range, and giving a near real time feedback of the obtained results, while keeping costs at a minimum compared to traditional methods using ships or buoys. [1, 2, 9, 11, 14, 15]

2.1.3 APPLICATION

With the continuous development in underwater glider technology, the applications of these vehicles are also expanding. From the passive Swallow float [4] reporting the velocity of an ocean current at a certain depth, to the more advanced commercial underwater gliders currently in service [1, 11, 14, 15]. These gliders mainly report salinity and temperature as a function of depth, position and time using CTD (Conductivity, Temperature, Depth) sensors plus GPS navigation at surface and dead reckoning while being submerged. Further developments can be seen in the examples presented in [16-18] with novel propulsion systems and functionalities. Some of these are capable of physical sampling, photographical sampling, and can carry an array of other sensors in addition to the common CTD. The applications of underwater gliders presented in this thesis cover some of the available functionalities and are not intended as a comprehensive list. However, since sampling and sensor

capabilities are not part of the scope of this project they will not be discussed in further detail.

Understanding the operational aspect of the underwater gliders, however, is imperative to developing a successful propulsion system. There are two main categorical approaches for surveying with an underwater glider; the first is to move across sections of the ocean; whereas, the second is to maintain a horizontal position by countering currents; acting as a virtual mooring. The main restriction of both of these methods is that the depth average velocity of a current must not exceed the horizontal velocity of the underwater glider. Consequently, the strength of the low speed and long range of an underwater glider also becomes a drawback, since the horizontal velocity of 0.25 m/s for an underwater glider is not uncommon for an ocean current either. One possibility to overcome this problem is to plan an underwater gliders mission to take advantage of the ocean currents instead of trying to counteract them. In the open deep oceans, however, the depth averaged velocity of the currents seems to be smaller than that of shallower waters, and the challenge is consequently reduced. Deeper operation presents another challenge, as the design of a buoyancy drive for operation in water deeper than 3000 m becomes increasingly difficult due to pressures exceeding 300 Bar [17]. Based on the studied literature, the operational depths of underwater gliders have yet to exceed this depth. Consequently, it would be beneficial for a propulsion system for underwater gliders to have both the opportunity to increase the speed, and the ability to go deeper. [1, 2, 11, 14, 15, 17]

2.2 HULL DESIGN

It can be argued that, for an underwater glider, creating more buoyancy generates greater forward propulsion for a given hull design within certain boundary conditions. A greater creation of buoyancy requires the conversion of more energy, which often is of limited supply due to storage constraints within the hull of the underwater glider. Moreover, a more efficient hull design will result in more forward momentum at a given buoyancy change. Consequently, the range of the vehicle can be stated to rely

much on these three factors, the hydrodynamic and hydrostatic efficiency of the hull, the energy density of the energy storage, and how efficiently this stored energy is converted into buoyancy change. The energy storage is further described in chapter 2.4, whereas the two first factors are covered in the following paragraphs.

2.2.1 HYDRODYNAMIC PERFORMANCE

As mentioned, the hull of an underwater glider is indisputably important in the development of underwater gliders. Whether it is speed, range, accuracy, or manoeuvrability; the hydrodynamic characteristics of the hull play a significant role. Accordingly, studies to determine and improve these characteristics have been performed from the very beginning of underwater glider development [7]. With the development of most underwater gliders follows a study of its hull design [11, 14, 15]. Also, studies focused on the underwater glider parameterisation and control alone have been performed [9, 19].

2.2.2 HYDROSTATIC PERFORMANCE

It is not only the hydrodynamic performance of the hull that is vital to determine the efficiency of an underwater glider; also the hydrostatic performance plays a significant role. As an underwater glider dives, it moves through waters that change in density due to compression. Consequently, an essentially rigid hull having neutral buoyancy at the surface will have increasing positive buoyancy, as it moves deeper in the compressible seawater. As a result, to be able to dive solely based on buoyancy, a rigid hull needs to achieve a larger negative buoyancy to efficiently reach greater depths. This results in the need for a larger increase in buoyancy for the underwater glider to ascend to the surface. Ultimately this leads to less efficient propulsion, as an underwater glider is propelled solely by the force created by the buoyancy change. A successful attempt has been made to simulate the compressibility of seawater in the underwater glider hull in the Seaglider [14], yet at a higher economical cost than conventional pressurised hulls [15].

2.2.3 SUMMARY

This thesis will not further discuss the properties of the hull, regardless of the importance of the subject. This is due to the absence of a tested hull at this stage of development and that the focus of the research is in the development of a novel propulsion system, or buoyancy drive. Consequently, to be able to compare the performance of the buoyancy drive to that of buoyancy drives used in other underwater gliders, characteristics of the commercial underwater glider Spray, as presented in [1], will be used for comparison. This will be more closely presented later in this thesis.

2.3 EXISTING BUOYANCY DRIVES

The term buoyancy drive refers to the buoyancy driven propulsion systems of underwater gliders. Several different buoyancy drives have been developed and tested, as presented in [1, 7, 11, 14-16, 20]. The convention is an electrically powered hydraulic system, as in the commercial underwater gliders Spray, Seaglider, and Slocum Battery [1, 7, 14, 15]. Though there are other competitive alternatives, as in Slocum Thermal [11]. Also a combination of a thermal engine, as in Slocum Thermal, using the waste heat of a Proton Exchange Membrane Fuel Cell (PEMFC) has been developed [16].

2.3.1 BATTERY POWERED

The battery powered propulsion systems all use electric motors to power hydraulic pumps that inflate and deflate bladders on the outside of chambers of constant volume which are isolated from the external pressure. As a result, the external volume of the underwater glider increases or decreases while the mass remains constant. Thus there is a corresponding change in buoyancy and consequently thrust, as explained in chapter 2.1.2. This high pressure pumping can result in gas bubbles forming in the hydraulic liquid. When using a small reciprocating pump, the volumes per revelation of the pump, and the corresponding amount of gas it can handle, are accordingly small. This phenomenon is referred to as vapour lock, and it

may prevent the pumps from working. The use of a single piston displacement pump eliminates this problem, but the pumping becomes more energy intensive. [1, 2, 7, 14, 15]

The aforementioned chamber of constant volume that the hydraulic fluid is pumped in and out of is essentially a pressure vessel functioning as an accumulator. Whether it has a positive, negative, or alternating charge pressure compared to ambient conditions, pumping the liquid in and out will require a modest yet significant amount of work at some stage to complete a cycle. A larger chamber may decrease the work yet require a larger mass of the vessel at a given pressure, and vice versa. When multiplying the efficiency coefficients in all the steps from energy source to buoyancy, the result is an inefficient system. It becomes apparent that a multi-stage conversion like this is not preferable when the goal is to make use of as much of the energy as possible. [1, 2, 7, 14, 15]

Although these systems are slightly inefficient, the battery powered underwater gliders show modest energy consumption compared to that of most other AUVs using propellers or water jets as propulsion. Not because the hydrodynamic efficiency is significantly higher as such, but simply because a lower operating speed becomes practically achievable [1, 2, 21]. This, along with a modest sensor load and efficient communication enables an underwater glider to have an impressive range and endurance. As an example, the commercial underwater glider Spray can cover up to 7000 km or endure 330 days without human intervention or the use of costly ship time [1]. This is possible by using 52 primary DD lithium CSC cell batteries weighing a total of 12 kg and storing 13 MJ at a cost of USD2850 per set. Also Slocum Battery and Seaglider make use of primary cell batteries and exhibit impressive endurance. The added cost of the primary cell batteries compared to that of rechargeable batteries is justified due to the extended endurance it provides. [1, 2, 7, 14, 15]

2.3.2 THERMALLY POWERED

Possibly the most astonishing solution is seen in Slocum Thermal, harvesting its propulsion energy from the ocean in which it operates [11]. It was intended to be the propulsion system of choice for underwater gliders and was in development at the

same time as the first test trial of the Slocum glider in 1991. The thermal buoyancy drive is based on the volumetric expansion and contraction of melting and freezing of the working fluid. The thermal cycle only has an efficiency of approximately 3% due to the small temperature difference, but because of the virtually unlimited source and sink of heat this does not present a significant limitation. The vehicle is limited only by the batteries that power the control system and scientific payload, or a possible failure, and it is indicated to have up to 30 000 km range [2]. However, since it is relying on a temperature difference from surface to bottom of at least 10ºC, it is not functional in Polar Regions, as well as certain regions/seasons of the temperate oceans. Also shallow operation presents a limitation. [11, 16]

2.3.3 FUEL CELL POWERED

Another approach is to use hydrogen fuel cells, which in functionality can be similar to the battery powered equivalent or be used in cooperation with a thermal engine. This is not a novel concept in underwater vehicles. In 1980 mature attempts at powering submarines by the use of fuel cells was underway by Siemens in Germany [22]. Promising prospects [23] for the use of PEMFCs in AUVs includes over 60% efficiency, neutral buoyancy, and low thermal signature. Surprisingly, although verifying the efficiency and low thermal signature of PEMFCs reported in [23], another study [16] presents the development of an underwater glider propulsion system making use of the waste heat of a PEMFC to power a thermal engine similar to the one used in Slocum Thermal [11]. This may seem like a promising system, yet similarly to Slocum Thermal it will be limited by the storage of hydrogen and oxygen to provide sufficient energy to the control system and scientific payload, as well as providing sufficient waste heat to power the thermal engine. Considering electrical power outputs of 50-150 W over a period of approximately 30 min per cycle as stated [16], the energy needed is substantial given an efficiency of a PEMFC in the range of 60%. Additionally it is also a comparatively complex system. Consequently, a fuel cell powered system may be competitive, but this has yet to be realised in practice.

2.3.4 STRENGTHS AND LIMITATIONS

The presented buoyancy drives for underwater gliders show impressive performance with ranges of up to 7000 km for battery power, and 30 000 km for thermal power [1, 2]. Nevertheless there are some limitations to be seen. They are highly dependent on working pressure, and show limited efficiency in the usage of the onboard energy storage. Slocum Thermal is not limited by the size of its energy supply but it is limited by seasonal and geographical conditions. The identification of these limitations led to the development of the proposed design.

2.4 CHEMICAL BUOYANCY DRIVE

The development of a novel propulsion system may start with the determination of desired characteristics. The use of a power source to directly generate buoyancy would eliminate the losses associated with conversion of energy from one form to another. Gravimetrically dense energy storage with a density and compressibility similar to that of seawater would further contribute to the efficiency of the system. Moreover, a flexible power output would enable long range in the open ocean, as well as enabling satisfactory operation in the higher velocity coastal currents. Finally, keeping the concept simple and partially independent of pressure will enable development of an attractive and functional system within the constraints associated with underwater gliders.

Many chemical reactions result in a direct volume change, such as the oxidisation of hydrogen and carbon from hydrocarbons in a conventional combustion engine. These reactions rely on the available gaseous oxygen in the air, which for obvious reasons is not readily available beneath the ocean surface. However, there are several reactions resulting in volumetric expansion that can occur in this environment. One is the hydrolysation of chemical hydrides, where the volumetric expansion occurs mainly due to the release of gaseous hydrogen from the chemical reaction between hydride and water. Consequently this results directly in buoyancy, since the released hydrogen is positively buoyant. Moreover it also makes use of some of the hydrogen present in the water as will be presented more closely in

chapter 2.5.1. In addition to this, the density of the different chemical hydrides range from slightly less dense to more dense than water, thus making it possible to achieve neutral buoyancy. Another potential aspect which is further explored in chapter 2.4.3 is the suspension of the chemical hydrides in an inert liquid media as slurry, eliminating the need to isolate the energy source from the external pressure. Suspension in slurry even gives the potential of an energy source with similar compressibility to that of seawater. Finally, as the whole concept is based on a single chemical reaction between the surrounding water and one reactant it seems practically obtainable to achieve simplicity of design.

The prospect of using a chemical hydride does seem to fulfil most of the previously described desired properties of a propulsion system for an underwater glider. Consequently this concept is further pursued, and a thorough investigation is presented in the following chapters.

2.4.1 CHEMICAL HYDRIDES

As with many of the alternative methods of storing hydrogen, the storage in chemical hydrides has received great attention in the last few decades. Furthermore, among the various alternative methods of hydrogen storage it may be considered as one of the more mature technologies. The volume of available literature on the subject is enormous, and there is a vast variety of studied hydrides and corresponding technologies. Due to this variety, the definition of a hydride is vaguely defined. The term hydride is widely used for both a hydrogen anion, and various compounds containing hydrogen. However, in this thesis the term hydride will refer to a compound consisting of hydrogen chemically bonded to metal, and it is these chemical hydrides that are of interest in this thesis. The chemical hydrides can be further divided into simple hydrides and complex hydrides. Simple hydrides consist of one host metal, typically from group 1 or 2 in the periodic table of the elements, bonded to respectively one or two hydrogen atoms (for example, lithium hydride {LiH} or magnesium hydride {MgH$_2$}). Complex hydrides refer to a metal bonded to a cluster consisting of another metal and hydrogen, typically also a metal from group 1 or 2 bonded to respectively one or two metal atoms from group 13 in the periodic table which is bonded to 4 hydrogen atoms (for example, lithium aluminium hydride

{LiAlH$_4$} or magnesium borohydride {Mg[BH$_4$]$_2$}). Due to mass requirements in hydrogen storage, the metals from period 2, 3, and 4 in the periodic table are of greatest interest. Several other complex hydrides exist (such as sodium aluminium hydride {Na$_3$AlH$_6$}) [24, 25].

2.4.2 SELECTION OF SPECIFIC CHEMICAL HYDRIDE

A survey based on the studied literature [24-45] has determined the preferred hydride for the intended use. The chemical hydrides presented in Table 1 are selected due to a gravimetric hydrogen content exceeding 15%. The beryllium hydrides have not been considered suitable due to toxicity and are therefore left out of the presentation [24]. Lithium borohydride {LiBH$_4$} and LiAlH$_4$ are considered unsafe due to their highly corrosive and irritant nature [46]. Further, MgH$_2$ is considered difficult to control due to passivation when reacted with water [39]. Other potentially interesting hydrides have been disregarded due to the lack of available literature, such as the complex aluminium borohydride {Al(BH$_4$)$_3$} being a liquid at ambient conditions exhibiting 17% gravimetric hydrogen density and the highest known volumetric density of 150 kg/m^3 [24]. Table 1 comprise a summarised qualitative comparison of a selection of chemical hydrides based on references [24-45].

TABLE 1: COMPARISON OF CHEMICAL HYDRIDES

	LiH	MgH$_2$	LiBH$_4$	NaBH$_4$	Mg(BH$_4$)$_2$	Ca(BH$_4$)$_2$	LiAlH$_4$
Weight % hydrogen	25.4	15.3	37.0	21.3	29.2	23.1	21.2
Reacts with water	Y	Y	Y	Y	N	U	Y
Reasonably safe	Y	Y	N	U	U	U	N
Easily controllable reaction	Y	N	U	U	U	U	N
Readily available literature	Y	Y	Y	Y	U	N	Y
Hydrogen yield under pressure	Y	U	U	U	U	U	U

Y=Yes, N=No, U=Unknown

From Table 1 it becomes apparent that among the suitable chemical hydrides, LiH is the most promising candidate based on the set criteria. It has high gravimetric hydrogen content, it does react with water, it is considered relatively safe, and the reaction is easily controlled. Moreover LiH, and the reaction product lithium hydroxide {LiOH} already present in seawater, are not regarded to be particularly toxic, or exhibit adverse environmental effects [46, 47]. Also of importance is the readily available literature both on the physical nature of the hydride, and on previous studies on the reaction between LiH and seawater at high pressure in similar applications [28, 45]. Additionally there are available studies of LiH suspended in slurry [28, 32, 35].

2.4.3 CHEMICAL HYDRIDE SLURRY

Slurry can be defined [32] as "a mixture of a solid and a liquid to make a pumpable mixture." Suspending the LiH in a liquid media to form slurry both eliminates the need for isolation from external pressure, and facilitates the control of reaction. LiH represents an explosion hazard in large quantities if not suspended in slurry [28], due to the high reaction rate, high heat of reaction, and creation of hydrogen. McClaine seems to be a central figure in the extensive work done on hydrogen storage in chemical hydride slurries funded by the US Department of Energy (DOE) hydrogen program [32, 35, 42]. Their early work presented in 2000 reports the development of a successful hydrogen generation system using LiH in light mineral oil [32]. This work, along with the work published in 1965 by deVries at the Bureau of Naval Weapons [28] is of great interest for the development of the buoyancy engine presented in this thesis. Experimental data [28] have been presented verifying the complete reactivity of LiH and seawater to a depth of 800 m. It is further shown that slurries of LiH suspended in various liquids exhibit equivalent hydrogen yields to that of plain LiH particles at complete reaction. Moreover it is shown that reaction rate can be controlled by altering grain size of the LiH, as well as the amount and type of liquid media used in the slurry [28, 32]. It is worth noting that the results presented [28] show significant variability between seemingly similar experiments. Moreover the results [32] are expressed without exhibiting precise values. Nevertheless, the two reports are considered to verify the functionality of the concept presented in this thesis.

2.4.4 GENERATION OF ADDITIONAL ENERGY

Hydrogen possesses several appealing properties. It is nontoxic and releases 142 MJ/kg, which is more than three times that of liquid hydrocarbons [33]. The energy is released by reaction with oxygen, either through combustion or by use of a fuel cell [32, 33], only giving off water as the product of reaction. These properties make hydrogen a very attractive energy carrier for onboard energy storage in mobile applications. Hence the opportunity to further use the generated hydrogen to fuel a hydrogen fuel cell becomes apparent. It is shown that the purity of hydrogen generated from LiH slurry is well within the requirements for efficient use in a PEMFC [32]. Further the volumetric density of hydrogen in an easily pumpable 60% LiH mineral oil slurry reacted with water is 118 kg/m^3 releasing 3937 Wh/l, and a gravimetric density of 5110 Wh/kg or 15.3% hydrogen [32]. Due to hydrogen being a low molecular weight gas with a critical temperature of approximately 33 K, it is difficult to achieve a competitive volumetric density in its pure form [48]. Consequently, the storage in LiH slurry compares attractively to the storage of hydrogen as liquid, or as compressed gas. Liquid storage does provide a compact energy source of 70.8 kg/m^3, yet the equipment to keep the hydrogen below 33 K is relatively complex and expensive [33]. Compressed hydrogen can be stored in carbon fibre composite pressure vessels achieving working pressures up to 450 Bar, yet still only achieving 4% hydrogen by mass in the system. Additionally, the storage of large volumes of highly flammable gas at 450 Bar is not without inherent risk [33]. Comparatively, the LiH slurry has been shown to be prevented from igniting due to the high vapour pressure of the mineral oil used in the slurry. Moreover, the mineral oil also prevents the LiH from reacting with moisture in the air [32].

2.4.5 CONCEPTUAL DESIGN

The proposed buoyancy engine uses the hydrolysation of a chemical hydride to generate hydrogen and resultant buoyancy. Since it is a chemical reaction that drives the buoyancy change, the buoyancy engine has been aptly named Chemical Buoyancy Drive (CBD). This chapter presents a conceptual description which does not include any additional functionalities or sub systems, and is intended to be an educational model more than an actual design drawing. It is worth mentioning that the presented model will only be efficiently functional for neutrally buoyant slurry.

Figure 2 on the next page gives a schematic view of a full cycle of the CBD from surface to bottom and to surface again, where **LiH slurry** has been used as fuel (**bold** indicates reference to the figure). The positively buoyant underwater glider at surface has the **reaction vessel** filled with H_2 from the previous cycle, as shown in Figure 2a. Further it is worth noting that the **slurry delivery** piston assembly is depleted of **LiH slurry** to the extent needed at the depth and speed of the previous dive. The piston is to be spring loaded to ensure that in any scenario where the normally open solenoid holding it were to lose its signal fuel is delivered resulting in resurfacing of the underwater glider (other methods to achieve fail safe functionality by resurfacing can be considered). Similarly, the **control operated valve** on the **reaction vessel** is normally closed to contain the buoyant hydrogen. Before ascent can be initiated, the **slurry delivery** system will need to be fully re-charged, as shown in Figure 2b where the movement is indicated by **arrow 1**. The charging of the **slurry delivery** system results in a decreased volume of the neutrally buoyant slurry left in the **slurry storage**. This volume will automatically be filled by sea**water**, as shown with **arrow 2** by the open inlet to the **slurry storage**. The flexible **slurry storage** is in concept a wet section separated from the seawater by a metal bellow, flexible bladder, or floating piston, as shown here. All three alternatives have previously been shown to be successful in similar applications [5]. Once recharging is complete the **control operated valve** is opened, flooding the **reaction vessel** with seawater through the bottom inlet, as indicated by **arrow 3**. Once the **reaction vessel** is flooded, the **control operated valve** will close, and the underwater glider dives to its predetermined depth.
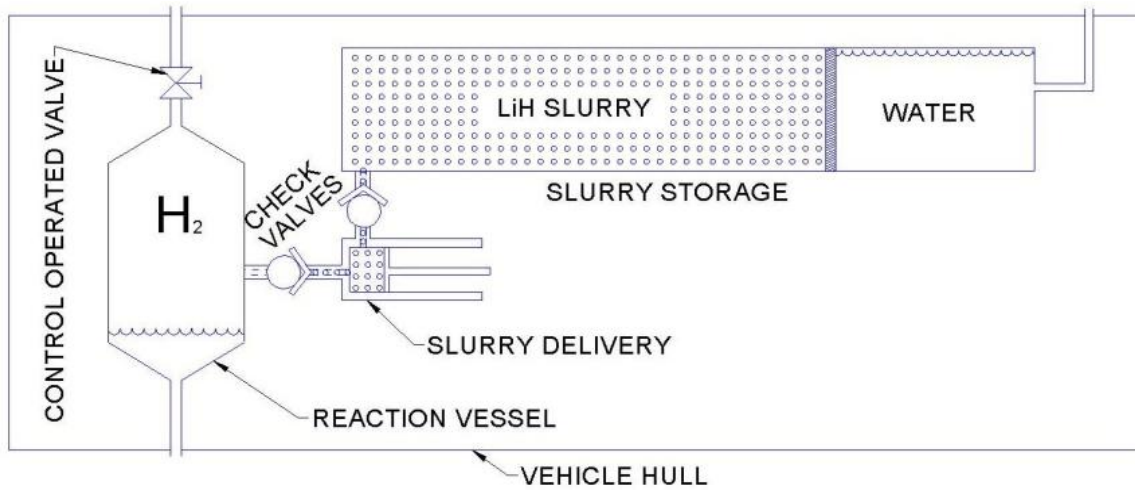
a) At surface the reaction vessel is filled with H_2 from the previous cycle giving positive buoyancy
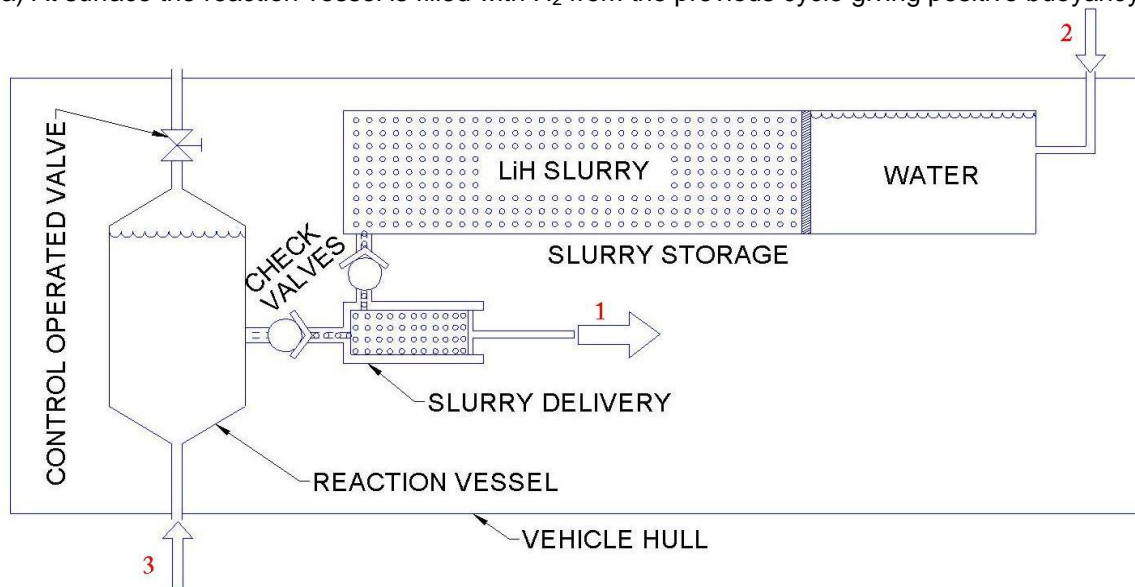
b) To initiate descent the slurry delivery is re-charged and the reaction chamber is flooded
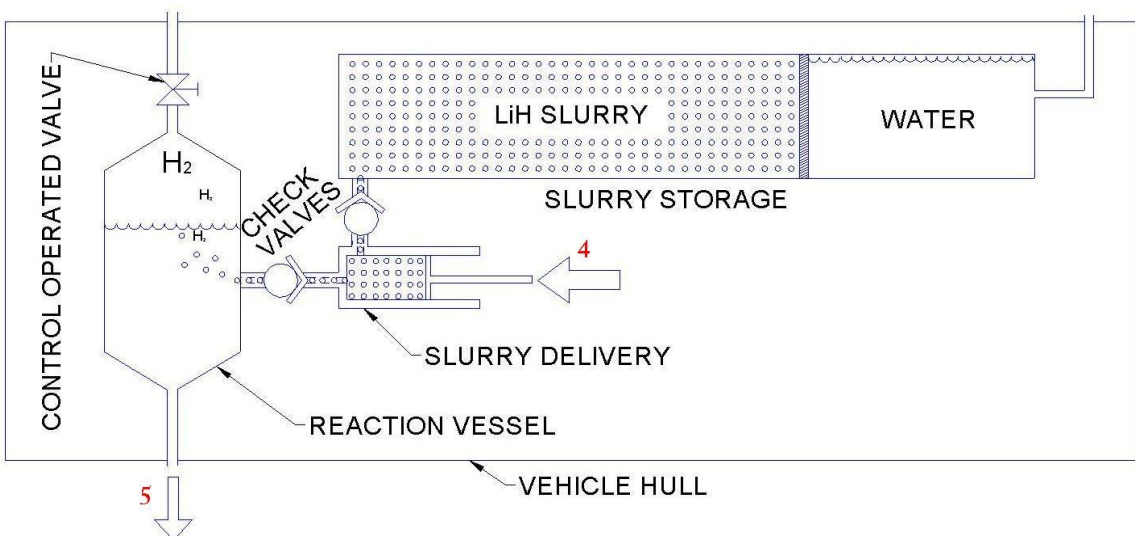
c) At bottom depth the slurry is delivered initiating the chemical reaction generating hydrogen expelling the seawater from the reaction chamber resulting in positive buoyancy and ascent.

FIGURE 2: COMPLETE CYCLE OF CBD

When this depth is reached the **LiH slurry** will be delivered by the **slurry delivery** into the **reaction vessel**, as shown by **arrow 4** in Figure 2c, instantly reacting with the seawater. The reaction generates **H$_2$** which will expel the seawater and the negatively buoyant hydroxide through the open outlet in the **reaction vessel**, as shown by **arrow 5**. Once the reaction is completed, so is the cycle, resulting in positive buoyancy, as shown in Figure 2a. The underwater glider will ascend until it reaches the surface, and the cycle can be repeated. The CBD shown schematically in Figure 2 on the previous page is, as mentioned, a simplistic conceptual design. The presented open design will function independently from pressure. It is dependent on neutrally buoyant **LiH slurry** and a sufficiently large slurry delivery system for the pressure at operating depth. Although this thesis presents the use of LiH specifically, the concept should be functional for essentially any chemical hydride that reacts in a similar manner with seawater.

2.5 PHYSICAL CHARACTERISTICS OF THE REACTION

To be able to determine the efficiency of the CBD it is necessary to accurately be able to quantify the physical phenomena involved. These phenomena include the reaction between LiH and seawater at elevated pressures, the compressibility of hydrogen, and the solubility of hydrogen and LiOH in seawater. Additionally, for the experiments presented in chapter 3.2, the density of LiOH solutions at various pressures along with the compressibility of seawater is of interest. All of these phenomena have been investigated and are presented within this chapter, either for water or seawater depending on available data from literature.

2.5.1 REACTION OF LITHIUM HYDRIDE WITH WATER

To be able to efficiently control the release of hydrogen it is important to know how the reaction between LiH and seawater proceeds. The reaction of LiH with water is an exothermic reaction that follows Equation 1 [28, 32, 45, 49], and it is indicated that this is also the case for LiH and seawater [28].

$$\mathbf{LiH + H_2O \leftrightarrow LiOH + H_2}$$
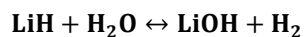
EQUATION 1: REACTION OF LITHIUM HYDRIDE AND WATER

However, although Equation 1 is correct seen as a whole, it can be further divided into two steps from beginning to completion. First, a fast reaction occurs, as shown in Equation 2.

$$\mathbf{LiH(s) + H_2O(l) \leftrightarrow LiOH(s) + H_2(g)}$$
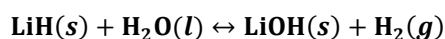
EQUATION 2: STEP ONE, REACTION OF LITHIUM HYDRIDE AND WATER [49]

Then, a slower reaction follows, as the LiOH dissolves in the water according to Equation 3.

$$\mathbf{LiOH(s) + H_2O \leftrightarrow Li^+(aq) + OH^-(aq)}$$
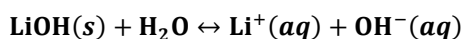
EQUATION 3: STEP TWO, DISSOLUTION OF LIOH IN WATER [49]

The solid LiOH is formed on the surface of the LiH, thus it is indicated that it may, to some degree, passify the LiH inhibiting the fast reaction between LiH and water. Nevertheless it is stated that with a large excess of water the reaction will proceed until completion [28, 45, 49]. The amount of excess water needed varies between the authors, but lies between 10 – 25 times the amount of LiH by mass. It is indicated that the passivation of the LiH becomes less prominent at elevated pressures [28], and it is stated that the rate of reaction in Equation 1 is highly dependent on surface area [28, 45, 49]. Correspondingly, the grain size of a LiH powder is influential on reaction rate [28].

Reference [49] reports that the reactions described in Equation 2 and Equation 3 are exothermic by 37 and 5 kcal/mol respectively, which roughly translates to a total of

175 kJ/mol Consequently, a significant rise in temperature is expected in both experiments and applied use. The accurate rise in temperature to expect in the experiment has not been determined, as the energy will be absorbed at different rates in hydrogen, water and the stainless steel reaction vessel. Further the experimental setup, as described in chapter 3.2.1, has not been insulated resulting in a transfer of thermal energy to the surroundings. Consequently, the mentioned calculation is deemed too complex to fit in the scope of the work presented in this thesis.

The reaction of LiH and seawater have, as previously mentioned, been proven to proceed at depths up to 800 m which translates to roughly 80 Bar [28]. However, to the author's knowledge there have been made no indications as to where the reaction ceases to occur. Accordingly, since commercial underwater gliders today are able to reach depths exceeding 800 m, an accurate determination of the reaction characteristics at higher pressures should be performed. The results of such a study would be of utmost importance to prove the feasibility of the proposed buoyancy drive as a competitive design to the existing systems.

2.5.2 EQUATIONS OF STATE

To determine the amount of generated hydrogen beneath the surface of the ocean, an accurate determination of the compressibility of hydrogen is paramount. At pressures and temperatures of pure gases close to standard conditions, the ideal gas law has an acceptable accuracy for most gases in most applications. The ideal gas law is shown below.

$$P * V = n * R * T$$

EQUATION 4: IDEAL GAS LAW

However, as pressure increases, the ideal gas law breaks down and becomes less indicative. Consequently, a survey of the well-known equations of state has been undertaken. The Van der Waals equation of state accounts for both repulsive and

attractive forces between gas molecules. Although sensible in principle it has been proven to have a largely variable accuracy for different media and conditions [50]. Other well known semi-empirical equations of state include Virial, Berthelot, Dieterici, Redlich-Kwong, Beattie-Bridgeman, and Benedict-Webb-Rubin [51]. Most of which have seen modifications to improve their accuracy. As these equations have varying accuracy at different applications, it is difficult to determine which one is the most accurate for a given application without experimental data [50, 52]. Reference [53] presents a thorough evaluation of equations of state and experimental data specifically for hydrogen at a wide range of pressures and temperatures. The results from [53] have been interpreted and presented in a comprehensive manner by National Institute of Standards and Technology (NIST) in reference [54], with a stated accuracy for density in the applicable range within 0.04%. However, the presentation of the results from [54] makes them impractical for use in a flexible model, thus these results are only used for comparison of the mentioned equations of state. In Figure 3 beneath, a comparative calculation of density from 0-400 Bar at 25^0C for hydrogen is presented for the equations where applicable variables have been obtained [51, 55].
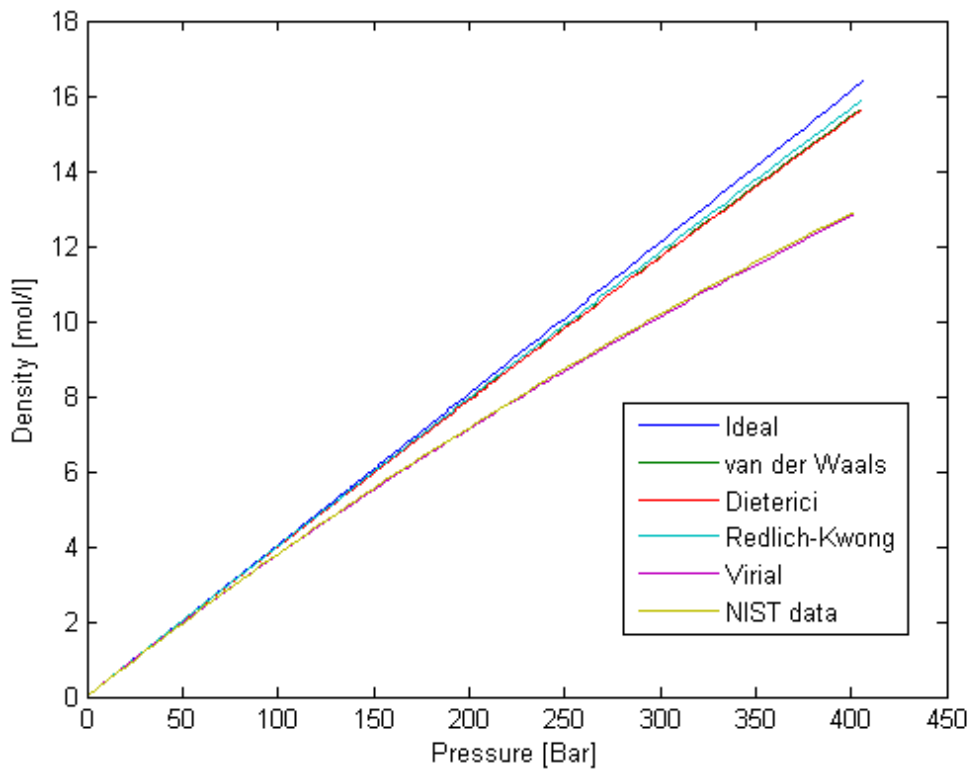
FIGURE 3: COMPARISON OF EQUATIONS OF STATE FOR HYDROGEN AT 25ºC

22

From Figure 3 a substantial variation of results can be seen at increasing pressures between the different equations of state. There is a clear correlation between the Virial equation of state and the data from NIST, and they deviate notably from the remaining equations. The constants utilised in the Virial equation of state is gathered from reference [55], which reports an accuracy of 0.5% for gaseous hydrogen from 25 to 600^0C and pressures up to 3000 Bar. The equation is shown below where a, b, c, d, e, and f are the gathered gas constants.

$$\frac{P*Vm}{R*T} = Z = 1 + \left(\frac{a}{T^2} + \frac{b}{T} + c\right) * P + \left(\frac{d}{T^2} + \frac{e}{T} + f\right) * P^2$$

EQUATION 5: VIRIAL EQUATION OF STATE

$$Deviation = \left|\frac{density_{virial} - density_{NIST}}{density_{NIST}}\right| * 100 \quad , [\%]$$

EQUATION 6: DEVIATION OF VIRIAL EQUATION OF STATE FROM DATA FROM NIST

Reference [55] states an accuracy of 0.5% or less for Equation 5 in the given range. However, since the work presented in this thesis will be performed in laboratory conditions at 21^0C, and may later be applied at 4ºC at sea, the accuracy of Equation 5 has been compared to the results presented in [54]. From Equation 6 the deviation has been calculated at 400 Bar for 25, 21, and 4^0C, and the results are shown in Table 2.

TABLE 2: DEVIATION FOR VIRIAL EQUATION OF STATE FROM DATA FROM NIST FOR HYDROGEN AT 400 BAR

25ºC	0.530	%
21ºC	0.541	%
4ºC	0.597	%

From Table 2 a relative error of less than 0.6% can be observed, and a tendency of increasing deviation with decreasing temperature may be concluded. This level of accuracy is deemed adequate for the intended use in the work presented in this thesis.

2.5.3 SOLUBILITY OF HYDROGEN IN WATER

In addition to the accurate determination of compressibility of hydrogen, its solubility in water at elevated pressures is of major concern to be able to accurately determine the volumetric expansion as a function of pressure. Reference [56] presents a comprehensive study for 0 to 100^0C and 25 to 1000 atm. The data is given as cubic centimetres of hydrogen at Standard Temperature and Pressure (STP) per gram water. Since it was published in the Journal of the American Chemical Society in 1934 it is assumed to follow the old UIPAC standard. This standard correlates with the current NIST standard and STP equals 0^oC and 760 mmHg of pressure. Figure 4 shows an interpolation of this data for 4 and 24^0C, which are the respective temperatures in the deep ocean and the laboratory.
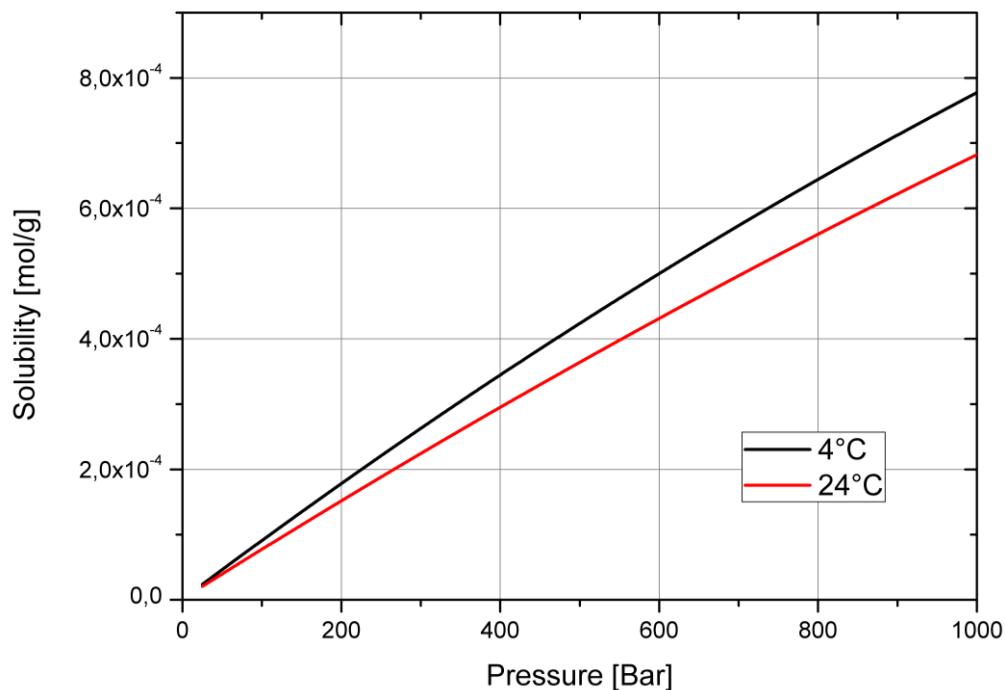
FIGURE 4: SOLUBILITY OF HYDROGEN IN WATER WITH PRESSURE

It is worth noting that not only does the solubility increase with increasing pressure and decrease with temperature in this range, but it also decreases with increasing salinity [57-59]. This however, has not been considered in the model since no good data has been found for elevated pressures in seawater. Similarly, the amount of hydrogen that may be dissolved in the water at depth remains unknown and has consequently been ignored.

2.5.4 DENSITY OF SALINE SOLUTIONS

The reaction of LiH with water generates both hydrogen gas and lithium hydroxide (LiOH). LiOH is soluble in seawater, thus the resultant density of this saline solution needs to be predetermined to be able to accurately determine the volumetric expansion of hydrogen. Reference [60] gives values for density of aqueous lithium hydroxide solutions at a range of temperatures and molar concentrations. The densities are compared to a theoretical calculation assuming zero solubility, and the results for 25ºC are presented in Figure 5.
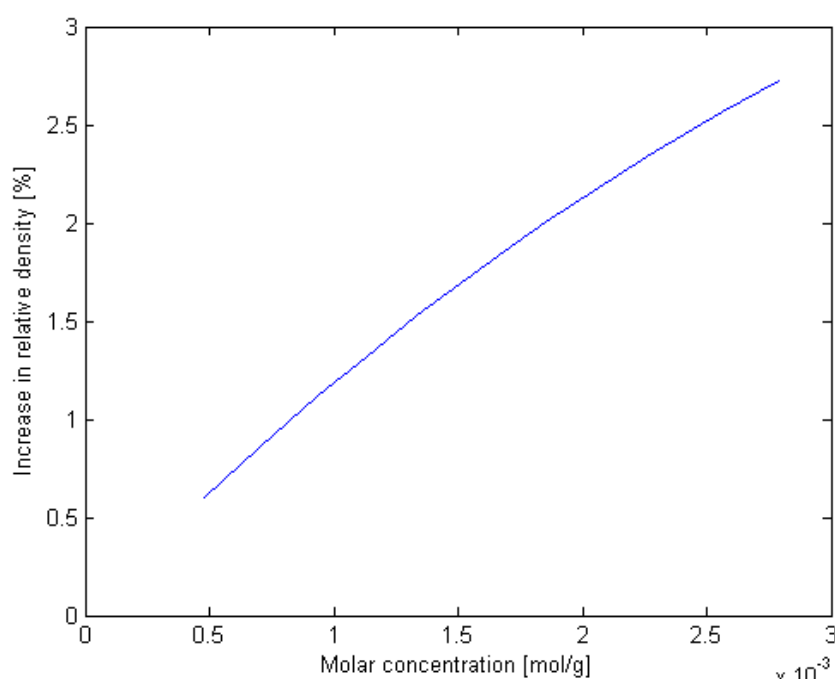
FIGURE 5: RELATIVE DENSITY OF AQUEOUS LITHIUM HYDROXIDE SOLUTIONS

From Figure 5 it can be observed that the dissolved LiOH occupies less volume resulting in an increase in density. The densities gathered from [60] are measured at a pressure of 1 atmosphere, nevertheless the values are considered to be indicative also for higher pressures. Moreover, although the results are given from a molar concentration of $4.8*10^4$ to $2.79*10^3$ mol/g due to the practically obtainable accuracy in this region, it is believed that the results can be extrapolated down to infinite dilution within reasonable accuracy.

2.5.5 COMPRESSIBILITY OF WATER

The compressibility of water will have an influence on the pressure increase from reaction, as the available volume for hydrogen will change with the compression of the water. The compressibility of seawater will influence the overall density of an underwater glider in terms of achieving neutral buoyancy, as previously presented in chapter 2.2.2. Reference [48] reports a relative volume of water at 0 and 10^0C for 1 and 500 atm. All of these four points fall within 0.9767 and 1.0001 relative to the volume at 0^0C and 1 atmosphere. However, the dissolved hydrogen and LiOH will have an influence on the experimental part, and the salinity of seawater will influence the applied part. For these reasons, along with the limited amount of data points in the area of interest for this research, the compressibility of water has not been implemented in the comparative and predictive theoretical model.

2.6 SUMMARY

This literature review has given an introduction to underwater gliders, their history and application. It has covered the basic functionalities of the buoyancy drives that are in use today, and their strengths and limitations have been presented. Based on these strengths and limitations a novel approach to underwater glider propulsion has been proposed. The feasibility of the proposed concept has been investigated based on available literature, and a conceptual design has been presented. It becomes clear which areas that are sufficiently explored, and which areas that will need further exploration to be able to develop the CBD.

The reaction of LiH with water and seawater, along with the applied use for hydrogen generation and storage using LiH suspended in slurry, are all relatively well known areas. However, the reaction characteristics of LiH with seawater at pressures exceeding 80 Bar are not. Consequently, the determination of reaction characteristics at conditions equivalent to those experienced by underwater gliders has become the main focus of the work presented in this thesis. The methods used to determine these characteristics are presented in detail in the following chapter.

3 EXPERIMENTS USED IN THE INVESTIGATION

To investigate the reaction of LiH with water and seawater at elevated pressures, a series of experiments of gradually progressing complexity have been performed. From the preliminary tests, where small amounts of powdered LiH were reacted with deionised water in an open beaker, practical experience with the reaction was obtained. Based on this experience, a conceptual model at atmospheric pressure using LiH slurry was built and tested. This was followed by a small scale pilot study investigating the reaction characteristics at elevated pressures.

Finally, a more complex experimental setup was designed and built. This was capable of determining the amount of hydrogen generated from the reaction at pressures up to and exceeding 300 Barg. Experiments were performed using both powdered LiH and LiH suspended in slurry, along with both deionised water and seawater in a range of test parameters. The experimental results obtained have been compared to the theoretical expectations presented in chapter 2.5 and calculated using a predictive mathematical model.

To verify the accuracy of these experiments and the theoretical model, this chapter presents their design, as well as how the experiments have been performed.

3.1 EXPLORING LITHIUM HYDRIDE

The reaction between LiH and water has been explored through a series of experiments. These experiments are presented in this chapter, starting with miscellaneous testing, through a conceptual laboratory model of the CBD, and finally a pilot study at elevated pressures.

3.1.1 MISCELLANEOUS EXPERIMENTS AT ATMOSPHERIC PRESSURE

As an initial approach to the testing, simple practical experiments with small amounts of LiH were performed to get some experience with the reaction and the effect of various reaction parameters. This initial testing involved dropping pure LiH powder

and LiH powder suspended in various liquids as slurry into an open beaker filled with water. The time of reaction was visually observed and recorded using a stop watch. The pH of solution was measured using pH-paper, and the temperature of the solution was measured using an alcohol thermometer.

Since the LiH is readily reactive with moisture, it was handled in an AtmosBag (Sigma Aldrich) under a dry nitrogen atmosphere whenever this was practically possible. Nevertheless, another test was performed to determine the yield of hydrogen at ambient pressures by reacting known amounts of LiH in a volumetric cylinder filled and inverted in water. The amount of hydrogen was visually read off and compared to the expected theoretical amounts, and a percentage yield was calculated.

The results from these miscellaneous experiments are presented in chapter 4.1.1 along with observations from the other experiments. In addition to the presented results, the initial testing resulted in valuable knowledge used in the development and implementation of the experiments presented in the following chapters.

3.1.2 CONCEPTUAL MODEL AT ATMOSPHERIC PRESSURE

The aim of this experiment was to quantify the reaction characteristics of selected slurry compounds at ambient pressure and temperature. It was acting as a proof of concept for the intended system being developed, and practical experience with the reaction was obtained before proceeding to experiments at higher pressures. Approximate reaction rate and volumetric expansion per unit weight of slurry was recorded.

The experimental set up shown in Figure 6 on the following page consisted of a modified 500ml wash bottle used as reaction vessel (**A.**), a syringe for delivery of reactant (**B.**), a glass beaker to collect the expelled water (**C.**), and a polyethylene tray to collect any possible spillage (**D.**). The vessel was made from polyethylene which was chosen for its excellent chemical compatibility with LiH and because it was translucent, enabling visual observation of the reaction. Moreover, it was not able to retain much pressure or break into hazardous shrapnel making it safe in case of a rapid rise in pressure. Although being sealed after it was partly filled with water it

would not withhold any significant internal pressure, as there was an open outlet in the bottom of the vessel. The LiH was supplied through a conventional syringe, and the reaction was instantly initiated, as it came in contact with the water already present in the sealed reaction vessel. The syringes were made from polypropylene and neoprene, which are believed to exhibit adequate chemical compatibility with the LiH slurries for this short term exposure. The reaction generates hydrogen, which results in the expulsion of water from the reaction vessel.
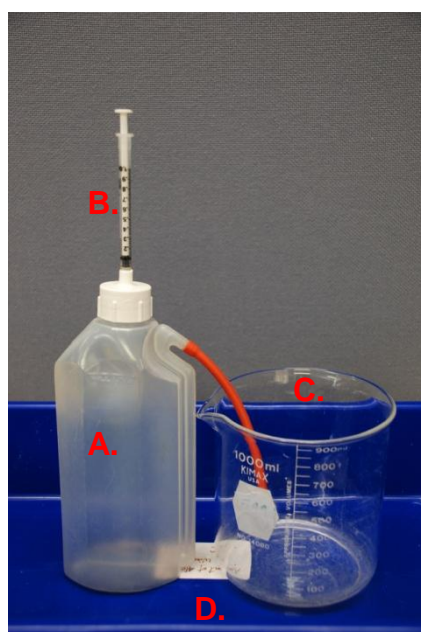
FIGURE 6: EXPERIMENTAL SETUP FOR AMBIENT PRESSURE

Several sources of error have been identified in the experimental equipment shown in Figure 6. The values obtained from these experiments are consequently not to be used as accurate values, yet they are believed to be adequately accurate to observe valuable trends in the reaction being explored. The identified sources of error are possible incomplete delivery of fuel, impurity of the LiH, expansion of non-rigid test vessel, dead space in outlet of system, slight increase in pressure and compression of hydrogen gas, and unknown temperature of hydrogen gas. These sources of error have not been contributed any significance, as they were believed to be similar for each test, and sufficient control was not feasible at this stage. The system was not touched between initiation and completion of reaction to ensure no external pressure

on the flexible reaction vessel that could aid the expulsion of the water, or provide externally initiated mixing of the reactants.

The apparatus was filled with 400ml tap water and the vessel was closed off. Following this, 0.1g LiH suspended in an inert liquid media was inserted using a syringe. This amount should theoretically expel approximately 310ml of water following Equation 1. The actual expelled water was collected in a beaker and the volume was recorded. An approximate time for completion of reaction was recorded using a stop watch. All points on the apparatus where leakage could occur were wetted with soap and water to indicate any leaks with the formation of bubbles.

3.1.3 PILOT STUDY AT ELEVATED PRESSURES

After testing had been done at ambient pressure and temperature and practical experience had been obtained with the reaction, a high pressure pilot study was performed. The study was based on a small volume reactor vessel, giving practical experience and a proof of concept at low risk and low cost.

The testing showed that a reaction did not cease to occur up to approximately 300 Barg which was the highest pressure of testing. However, due to the limited control over amount of supplied water and accurate time of reaction the quantified results have not been given any significance. Nevertheless, these experiments did give indications to the feasibility of the intended system, and the practical aspects of the process became better understood. Consequently, this pilot study resulted in the design and development of the experimental setup described in the following chapter.

3.2 HIGH PRESSURE EXPERIMENT

To successfully develop the proposed propulsion system an accurate knowledge of the amount of hydrogen generated from the reaction between LiH and seawater is paramount. This chapter presents the experimental setup used to quantify this hydrogen generation. The setup measures the increase in pressure in a sealed

reaction vessel, contradictory to the proposed system which expels water from the reaction vessel as a result of the generated hydrogen from reaction. Although the experiment could have been more similar in functionality to that of the CBD, it has been decided to do it like this to achieve a more stringent control of the contents of the reaction in a simpler almost static system. The stringent control of the contents enables a higher degree of accuracy, which is of utmost importance in the experiment presented herein.

3.2.1 EQUIPMENT AND SETUP

To determine the reaction characteristics of LiH with water at elevated pressures, a high pressure reaction system has been developed. It can be divided into four sections. These sections are referred to as the Water Supply and Data Recording, High Pressure Section, Hydrogen Supply, and Hydrogen Collection, and a picture of all four sections as a complete system is shown below.
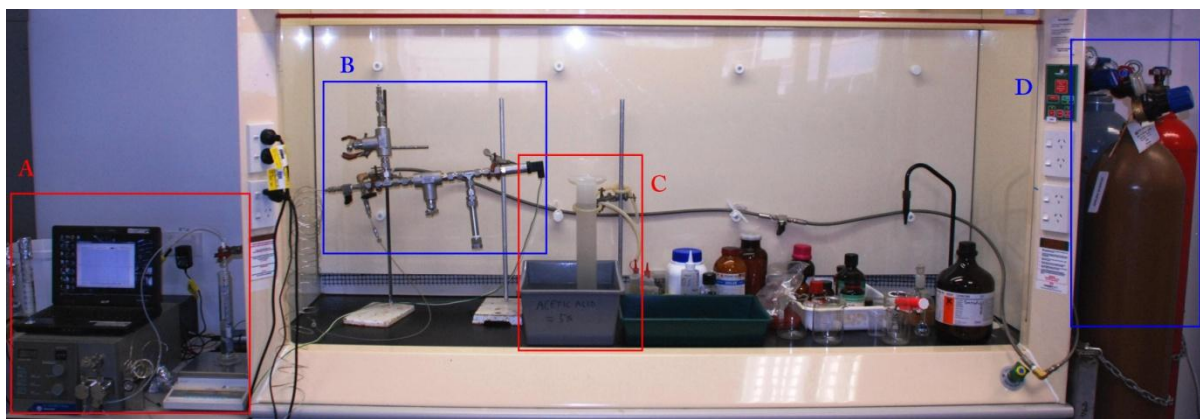
FIGURE 7: COMPLETE EXPERIMENTAL SETUP: A: WATER SUPPLY AND DATA RECORDING B: HIGH PRESSURE SECTION C: HYDROGEN COLLECTION, D: HYDROGEN SUPPLY.

The picture shows the components as they are situated and do not follow the logical order of which this text is written. This is due to the high pressure reaction system and hydrogen collection unit is kept within a fume hood, whereas the electrical components and gas supply are kept outside and separate, as can be observed in Figure 7. The reason for this is to extract the developed hydrogen safely through the

fume hood extraction fan after each test run without having any sources of ignition (i.e. electronic equipment) present. The pressure transmitter has for practical reasons been kept within the fume hood. Further description of the different sections of the experimental setup follows below.

High pressure section

In the high pressure section the LiH is reacted with water under pressures up to 300 Barg. A picture of the section can be seen in Figure 8, followed by a schematic in Figure 9.

FIGURE 8: PICTURE OF HIGH PRESSURE SECTION
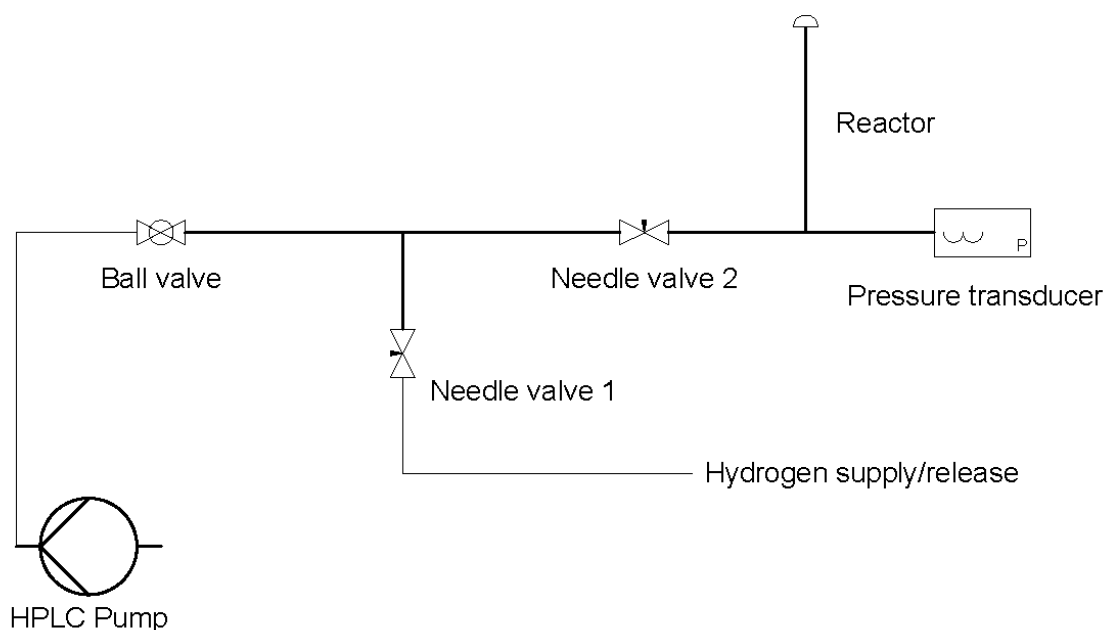
FIGURE 9: SCHEMATIC OF HIGH PRESSURE SECTION

The schematic above shows the main components of the high pressure section of the experimental setup. Since the High Pressure Liquid Chromatography (HPLC) Pump is situated away from the rest of the high pressure section it is not shown in Figure 8. A detailed list of the equipment and parts used can be found in Appendix D1.

The internal volume of the system has been determined by charging the system to a measured internal pressure, then releasing the hydrogen to a measured ambient pressure, and recording the expelled volume. A total of 12 tests were performed, of which 6 for the total internal volume, and 6 for the internal volume of the reactor only. For both volumes two tests were performed at 2, 6, and 7.75 Barg respectively. Results for these tests are presented in Table 3 below.

TABLE 3: INTERNAL VOLUME OF EXPERIMENTAL SETUP

	Internal volume [ml]	**Standard deviation [ml]**
Total	69.1	+/- 3.96
Reactor	45.5	+/- 2.49

34

Please note the significant standard deviation given in millilitres. The data processing limits the effect of this inaccuracy on the experimental results, as explained in chapter 3.2.4. The next section covers the hydrogen supply and collection that is connected to the high pressure section.

Hydrogen supply and collection

The high pressure system is purged and charged with hydrogen on each test. This way the compression rate is more accurately known, as there will only be one gas present. Moreover, this inhibits ignition of the hydrogen as a result of the heat generated in the exothermic reaction since there is no oxygen from the air present. As mentioned in 3.2.1 the hydrogen used is High Purity (Air Liquide) and it is regulated by a hydrogen regulator (Comet Cigweld) delivering approximately 0-7.75 Barg. Further details on this equipment are presented in Appendix D.

After each test the hydrogen is collected in a 500 ml measuring cylinder that is filled with dilute hydrochloric acid {HCl} and inverted in a bath of dilute HCl. The reason for using HCl instead of water is to neutralise the alkaline LiOH solution that is expelled from the reaction together with the hydrogen. The amount of hydrogen expelled is visually read off the measuring cylinder. It is worth noting that the internal volume of the collection line is filled with air at ambient pressure both before and after release, thus is not influential on the recorded volume. The internal volume of the high pressure section however is mostly filled with water before reaction, and hydrogen after the reaction, therefore it is added to the total volume read off the measuring cylinder. The recorded pressure of which the high pressure system was initially charged gives the amount of hydrogen supplied, and this is subtracted from the recorded volume after reaction. This represents the molar quantity of hydrogen generated from reaction.

Data recording

The pressure in the high pressure section is recorded through the course of a test run through a pressure transducer connected to a data logger which is further connected to a computer. The recorded results are analysed in MatLab using the

developed program as described in 3.3, and this MatLab code can be found in Appendix A.

The pressure transducer is powered by a battery, which voltage was regularly checked before, during, and after testing. This was to ensure that it could not influence the output of the pressure transmitter by a change in voltage as a result of an increase in load with pressure. Since the transducer gives an output signal of 4-20mA and the data logger records voltage, the signal has been converted by taking the subsequent voltage over a known resistance. A description of the components can be found in Appendix D.

Miscellaneous equipment and reactants

The remaining miscellaneous equipment along with the various reactants used in the experiments is presented in a list that can be found in Appendix D1.

3.2.2 TEST PROCEDURE

To ensure the results are as comparable as possible, a specific procedure for the performed experiments has been followed. A step wise checklist improved the success rate of the experiments; this list along with a procedure for the preparation of the system can be found in Appendix C. In addition to this list, an explanation of each step of the experiment is presented in this chapter.

Initial Pressurisation of the Reaction Chamber

After the system is prepared and the LiH is introduced, as explained in "High pressure experiment – Preparation" found in Appendix C, the system is pressurised with hydrogen from the hydrogen bottle until the system reaches equilibrium with the set outlet pressure of the hydrogen regulator. This pressurisation can range from 2 to 7.75 Barg depending on the specific test run. Once this equilibrium pressure is reached, needle valve 1 is closed leaving a sealed system. The hydrogen supply is then shut off and disconnected, and finally the internal pressure of the pre-charged high pressure section is recorded.

Introduction of Water and Further Pressurisation

After the system has been filled with hydrogen and sealed, the ball valve is opened, and the pump begins to fill the high pressure section with water. One reason for doing this is to reach a higher initial pressure of 12.5 to 300 Barg from compressing the hydrogen. Another reason is to introduce the water as the second reactant in the reactor. Based on values for hydrogen compressibility and solubility under pressure found in literature the measured increase in pressure is used to determine the amount of water present in the reactor. In addition to this the water supply is weighed before, during, and after charging is complete thus giving the amount of water supplied. Once the amount of water needed to reach the desired pressure is delivered, the pump is stopped and needle valve 2 is closed leaving the reactor sealed with water and LiH separated from each other by the compressed hydrogen. The system is left like this for approximately 5 min to let the hydrogen dissolve in the water leaving a system in equilibrium before initiating the reaction.

Initiation of Reaction

Once the system seems to be in equilibrium, the sample rate on the data logger is increased to more accurately record the rapid reaction between the LiH and the water. Shortly after the sample rate is increased, the high pressure section of the system is simply turned upside down letting the compressed hydrogen float to the other side of the reactor, as shown in Figure 10.
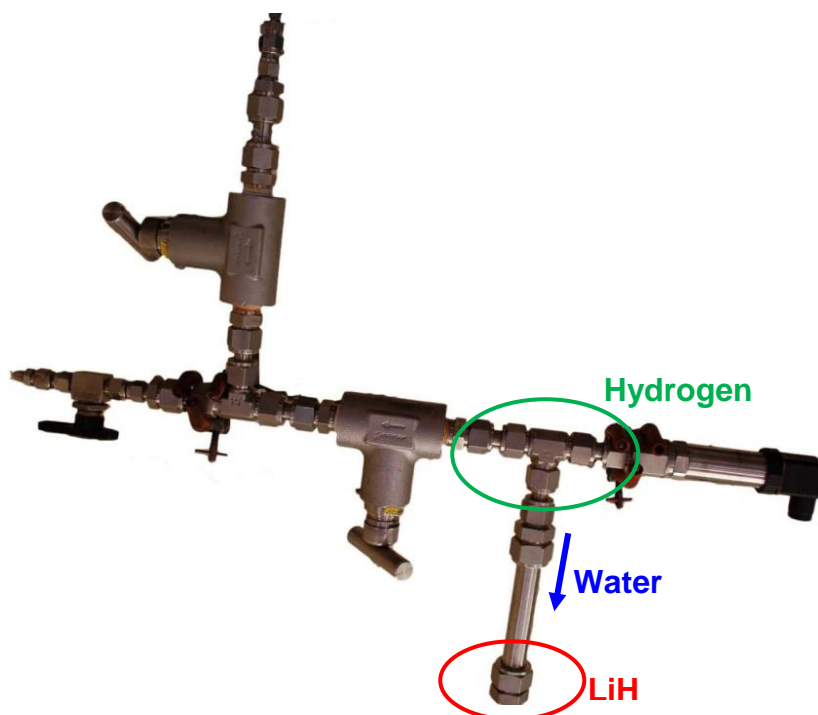
FIGURE 10: GRAVITY ASSISTED INITIATION OF REACTION IN THE HIGH PRESSURE SECTION

Hydrogen was the only thing separating the water and the LiH, so the water comes in contact with the LiH initiating the reaction and the increase in pressure is recorded. The subsequent partial loss in pressure due to higher hydrogen solubility at higher pressures is also recorded for approximately 5 min after reaction.

Depressurisation and collection of hydrogen

Once the reaction seems to be in equilibrium based on the pressure readings the high pressure section needs to be depressurised. Hydrogen, as opposed to most other gases, heats upon expansion. Consequently the rate of relief of the pressure needs to be controlled. Where the hydrogen supply was connected, the hydrogen collection hose is now connected. This hose is used to direct the released hydrogen to the measuring cylinder ready to collect the hydrogen, as explained in chapter 3.2.1 under "Hydrogen supply and collection". Once this hose is in place needle valve 1 can be opened to investigate whether there has been a hydrogen bubble trapped outside the reactor. When there is no flow needle valve 2 is opened and the pressure is released. The hydrogen is collected and the atmospheric volume is visually recorded to an accuracy of +/- 1ml. This volume is compared to the expected

amount of hydrogen to be expelled from the preliminary charging of the system, and the amount exceeding this is the volume that has been generated in the reaction.

The amount of hydrogen trapped outside the reactor ranges from one to eight millilitres at STP and is following the charge pressure. Since this accounts for approximately 1% of the total amount of hydrogen used for charging, it has been disregarded as an influence on the recorded results.

Once the presented steps are completed, the system can be cleaned, dried, and prepared for the next test.

3.2.3 PURPOSE OF EXPERIMENT

The purpose of this experiment is to account for most influencing parameters of the reaction between LiH and seawater. The results will be compared to the theoretical model described in chapter 3.3, and provide a platform to base the control of the proposed CBD upon in addition to setting the design parameters. Unfortunately not much accurate data have been found on the reaction between LiH and seawater compared to what is available for pure water. Consequently, the theoretical model depicts the expected reaction characteristics between LiH and water. To be able to validate the applicability for seawater, experiments for both water and seawater will be performed. As an additional reference for the effects of salt concentration a saturated sodium chloride {NaCl}-water solution could be used. Similarly, there is not much accurate data available for the use of LiH suspended in slurry. Consequently, tests for both pure LiH powder and LiH powder suspended in slurry is to be performed. To determine influences of the characteristics of the liquid used in the slurry more than one slurry-liquid will be tested. Additionally, not only the type of reactant, but also the quantity will have an influence on the reaction. Consequently, tests with different amounts of LiH to water and tests at different charge pressures are to be performed.

When there is more than one factor influencing the reaction characteristics also the amounts of tests increase as only one parameter should be changed at a time. However, when for instance the amount of LiH is the only changing input parameter, it will effectively change more than one parameter affecting the reaction. As an

example, increasing the amount of LiH will also affect the LiOH concentration in solution, the amount of dissolved hydrogen, the pressure change from reaction, and the temperature in the reactor. These factors could be anticipated prior to performing the experiment and the other parameters could be adjusted to account for these effects. However, this anticipation will only be an approximation thus accurately adjusting other factors will not be possible. Moreover, when adjusting other parameters then other factors will be affected and so on and so forth. Consequently, for simplicity's sake this will not be further accounted for. Changing one input parameter at a time will determine the impact of each parameter with adequate accuracy to depict the trends that are to be determined. The different test parameters are shown Table 4.

TABLE 4: TEST PARAMETERS FOR REACTION BETWEEN LIH AND WATER

	2/45 Bar	4/85 Bar	6/110 Bar	7.75/130 Bar	2/160 Bar	7.75/270 Bar
LiH [g]	0.025	0.025	0.025	0.025	0.025	0.025
	0.050	0.050	0.050	0.050	0.050	0.050
	0.100	0.100	0.100	0.100	0.100	0.100

The test parameters shown in Table 4 are a condensed depiction, leaving out the method of fuel delivery and type of water. For each amount of LiH, three tests should be performed with three different fuel deliveries. These are pure LiH, LiH suspended in Isopar L oil and LiH suspended in Mobil DTE Heavy Medium oil. Both oils should be mixed with the LiH in a 1:1 ratio by mass. Different ratios and liquids could also be tested, but this selection will give good indications of the expected effects of different suspensions. Additionally, each of these test series should be performed for both deionised water, sea water, and a saturated NaCl solution to indicate changes with changing salinities. A complete table of testing parameters can be found in Appendix C.

The pressure columns in Table 4 refer to charge pressure before the reaction is initiated. The specific pressures are chosen to give a wide pressure range while keeping the amount of water and volume of hydrogen constant in two separate

series. This is achieved by altering the initial hydrogen charge pressure of respectively 2, 4, 6 and 7.75 Barg pressure. The corresponding 45, 85, 110, 130, 160, and 270 Barg depicts the final hydrogen charge resulting from the amount of introduced water before reaction. Moreover, identical series for each parameter can be extracted, (e.g. same test parameters for both water and seawater). If all these tests are to be performed it will require 162 test runs times 1.5 h per test run, which equals 243 h of efficient laboratory testing. Additionally, if more than one test is to be performed per set conditions, the amount of hours will be multiplied accordingly. Due to time constraints in this project, this is not practically achievable. Therefore a selection of the test runs will be performed instead, and the results will need to be interpolated and/or extrapolated to determine the effects when applied to conditions that have not been tested. Similarly, the reproducibility will be determined for one set of conditions and the result applied to the remaining tests. The selected tests that have been performed will be presented in chapter 4.

3.2.4 IDENTIFIED SOURCES OF ERROR

In the experiment, some sources of error have been identified. These are presented below, starting with the influence of the measured internal volume of the reaction vessel. After the various sources of error have been accounted for, the accuracy of the experiment is discussed.

Internal volume

The accuracy of the measured internal volume of the reaction vessel is influential on the accuracy of the recorded results since it dictates the volume available for hydrogen after the addition of water. Due to complex internal geometry of the experimental set up it proved difficult to achieve an accurate measure of the internal volume, as presented in Table 3 under chapter 3.2.1. To counter this, the predictive model iterates to fit the internal volume based on a mix of the initial measured volume and the predicted behaviour of pressure rise with the addition of water. This approach will limit the offset of pressure due to an inaccurate internal volume, but unfortunately does not eliminate it completely. Such an offset is expected to increase with increasing pressures.

Volumetric expansion of reactor as a function of pressure

As internal pressure in the reactor rises, the reactor will be expanded and the internal volume will increase. Although intuitively the relative expansion is small, it has been investigated to accurately determine its effect on the experiments.

The pressure vessel was pressurised using hydrogen and water in the same manner as is done in the experiments. The external length of the reactor has then been measured at approximately 0, 40, 100, 200, 250, and 300 Barg. To measure this length a 150 to 300mm micrometer (Mitutoyo) with a stated accuracy of 10 μm was used. Two tests were performed for each pressure due to surface roughness on the reactor, and the mean of these values has been recorded. Despite an accuracy of 10 μm a value for 1 μm was recorded since this was visually achievable on the micrometer. This added accuracy does not indicate actual length of the reactor, but is believed to give an accurate relative change in length as the temperature was constant throughout the testing at 23.5^0C. The micrometer was calibrated using the reference rods supplied with the micrometer.

The change in length has been used to generate an expansion coefficient of $4.6505*10^{-7}$ annotated in [mm/Bar*mm] or [Bar^{-1}]. This results in a volumetric expansion of the reactor of 0.0246 ml from 0 to 300 Barg. This is regarded to be much smaller than the accuracy of the measured internal volume of the reactor. Consequently, the expansion is not taken into account in the theoretical model.

Hydrogen lost due to premature reaction

Charging of the system typically takes about 15 min of which the hydrogen from the bottle is able to absorb moisture from the water thus enabling reaction with the LiH slurry. Like the volumetric expansion of the reactor due to pressure, also this is believed not to be a major influence. Nevertheless, it has been explored to determine its effect.

To determine this effect the bottom of a glass measuring cylinder was painted with LiH slurry. It was then inverted in a beaker with water leaving it separated from the water with a few millilitres of air. After being left for an arbitrary amount of time which happened to be 165 min, 4.1 ml gas expansion was recorded. This gives an

estimated hydrogen generation rate of 0.0124 ml/min*cm^2 contact area of reaction at room temperature and atmospheric pressure. Compared to the total amount of hydrogen generated in the experiments this is not regarded as a major influence.

That being said, the experiments are performed using hydrogen instead of air, and pressures up 300 Barg instead of atmospheric pressure. Contrary the hydrogen used is initially dry, whereas the air on the day of testing had a relative humidity of 75%. Correspondingly, the experiment performed may not accurately reflect the hydrogen generation rate used in experiments, but it gives an indication of the magnitude of the effect.

Leak in experimental equipment

The experimental results are dependent on leakage of the experimental setup, as a leak would reduce the measured yield of hydrogen. As mentioned, the system has been checked using a leak detector on each test run. The tests that did exhibit any significant leaks have been discarded. In addition to this, leak tests were performed, and the results can be found in Appendix B1. Although there is a minute leak to be observed over the course of the leak test, it has been regarded as insignificant due to the comparatively short time span of a test run to that of a leak test, and the modest amount of leakage that was observed.

Accuracy of experiment

The accuracy of this experiment is a function of the effects from all the influencing factors. The accuracy of the pressure transmitter, the scales and other inaccuracies stated by the respective manufacturers of the experimental equipment used are of comparatively little influence, and will consequently not be further discussed. Technical information on the equipment can be found in Appendix D2. The amount of expansion of the reaction vessel with pressure and the amount of hydrogen lost to premature reaction have been determined. These factors have not been implemented in the data processing, since the effect expected to be less significant than the inaccuracy of the measured internal volume. Similarly, the effects of leaks that are too small to be detected with the leak detector have been disregarded. As

explained earlier in this chapter, the effect of the inaccurately determined internal volume has been limited in the MatLab code, yet it is still believed to be influential. How much influence these factors will have combined is difficult to determine, and it would require a complex mathematical exercise exceeding the scope of the research presented in this thesis. Consequently a calculation to determine a quantified accuracy has not been attempted.

3.3   THEORETICAL MODELLING

As a reference to the results from the experiment described in chapter 3.2, a predictive theoretical model has been developed through MatLab. It is based on the influencing parameters on the reaction presented in chapter 2.5. Although several studied influencing parameters are available from literature, the developed model relies on a set of assumptions. These assumptions are presented in chapter 3.3.1 below, followed by a brief description of the program in 3.3.2.

3.3.1 ASSUMPTIONS
In the development of the MatLab model a set of assumptions have been made:

- For simplicity in both the model and the experimental set up, the reaction is modelled as isothermal.
- The model assumes the non-polar liquids used in the slurry to be completely inert, immiscible with water and completely hydrophobic.
- Based on the relative amount, the slurry liquids have been assumed to not absorb any hydrogen or LiOH.
- The dimension of time has not been included in the calculations, hence the solubility of hydrogen and LiOH in water is assumed to reach instant equilibrium at any stage.

- The solubility of hydrogen in seawater is considered to be identical to that of deionised water even at elevated pressures due to a shortage in the studied literature.

Other than the given assumptions, the model is believed to accurately depict a complete stoichiometric reaction for the given conditions.

3.3.2 LOGICAL PROGRESSION

The program is based on the following logical progression. Firstly, the experimental raw data is imported along with input parameters of the reaction. From the data, isolated parts of the experiment are extracted, like the initial hydrogen charge pressure, the final charge pressure, and the input parameters. Based on these inputs the program computes the expected outcome of the reaction. Finally the observed experimental data for complete reaction and the calculated expected outcome are compared, and plotted for each test run along with comparative plots of multiple test runs. These plots and comparisons are presented in further detail in chapter 4.2 and 4.3.

To explain how this theoretical model works in much further detail than this will not be attempted, as it is expected to be more easily understood by reading the code directly. Consequently, the MatLab code presented in this chapter can be found in Appendix A.

4 FINDINGS FROM THE INVESTIGATION

The findings presented in this chapter will give a clear understanding of how the chemical reaction between LiH and seawater behaves as a function of pressure and other parameters. Experimental data has been recorded in the experiments presented in chapter 3, and various observations have been made. The observations have been summarised and described in chapter 4.1. The gathered data from the reaction of LiH with water and seawater at elevated pressures have been processed using the developed MatLab code, and been compared to the theoretical expectations. This has resulted in a series of graphs depicting the percentage completion, reaction rate, and pressure increase from reaction, along with the amount of generated buoyancy from experiments compared to theoretical expectations. These graphs are presented in chapter 4.2, followed by a theoretical prediction of the CBD performance at conditions exceeding the experimental results in chapter 4.3.

4.1 GENERAL RESULTS AND OBSERVATIONS

This chapter is a summary of the many observations that have been made through the course of this research. It will provide a general understanding of the chemical reaction being explored, cover the effects of slurry composition on the reaction, and propose potential challenges that may be met in the development of the CBD.

4.1.1 MISCELLANEOUS EXPERIMENTS AT ATMOSPHERIC PRESSURE

Several experiments have been performed before and during the more complex testing presented in chapter 4.2. These experiments have provided valuable practical experience with the reaction between LiH and water, and it has additionally verified the actual purity of the reactant at the time of experimentation. The results from these experiments are presented in the following paragraphs.

The reaction of powdered LiH in water at atmospheric pressure and room temperature proceeded to completion in less than 1 s in the amounts that were tested. These amounts varied but were all less than 1 g per test. The resulting LiOH solutions were significantly alkaline even at moderate amounts of reactant as expected.

When reacted in a high ratio of LiH to water temperatures reached 90^0C. Since the reactant was added gradually over approximately 2 min to limit spills due to an uncontrollable reaction, the ratio of LiH to water in this experiment is not accurately known. The response time of the alcohol thermometer can possibly have affected the measured temperature.

The percentage hydrogen yield from powdered LiH at atmospheric pressures was repeatedly measured to approximately 92%. This has been included in the comparative theoretical model and has consequently been accounted for in the results presented in chapter 4.2. This less than complete yield of hydrogen has been contributed to 95% purity of the supplied LiH, and degradation due to contact with moist air. It is worth noting that these tests were performed in between the high pressure experiments with the same batch of LiH, thus it should be presentable for the LiH used in the experiments.

From the experiments presented in this chapter it can be concluded that the reaction is rapid at atmospheric pressures, the resulting bi-product can be highly alkaline, and temperature can increase significantly. Based on these observations, caution is advised when handling LiH and reacting it with water. That being said, when treated with respect, the reaction is predictable and easy to control. The following chapter covers LiH suspended in an inert liquid as slurry and the reaction of this slurry with water.

4.1.2 SLURRY COMPOSITION AND ITS EFFECT ON REACTION PARAMETERS

As briefly explained in 3.1 various slurry liquids and mixing ratios have been tested and the reaction parameters have been recorded. The results are presented in Table 5.

TABLE 5: EFFECT OF SLURRY COMPOSITION

Water [ml]	LiH [g]	Delivery method of LiH	Time [s]	Alkalinity [pH]	Viscosity of slurry liquid [cP]	Comments:
600	-	Powder	<1	8-9	-	Strong effervescence
300	0.0067	Powder	<1	10-11	-	<1°C rise in temperature
500	0.0120	Toluene 1:20	1	-	-	
500	-	Isopar L 1:20	1	-	-	
500	-	Olive oil 1:20	60	-	-	
500	-	Glycerol 1:20	10	-	-	Reacts with LiH
500	-	Diesel 1:20	60-120	-	-	Unstable reaction rate
500	-	O-xylene 1:2	1	-	0.81 [cP@20°C]	Evaporates
500	-	M-xylene 1:2	1	-	0.62 [cP@30°C]	Evaporates
500	-	P-xylene 1:2	1	-	0.34 [cP@30°C]	Evaporates
500	-	Benzyl alcohol 1:2	1-2	-	8 [cP@25°C]	Reacts with LiH
500	-	Kerosene 1:2	1-2	-	1.96 [cP@40°C]	
500	-	Mobil DTE 25 1:2	3	-	38.7 [cP@40°C]	
500	-	Mobil DTE H/M 1:2	4	-	56.6 [cP@40°C]	High viscosity in this ratio of LiH

Blue: LiH powder　　　**Green: 1:20 (LiH:liquid)**　　　**Yellow: 1:2 (LiH:liquid)**

All the tests presented in Table 5 were performed at room temperature and at atmospheric pressure. The amount of slurry was not measured accurately in these experiments and is consequently not recorded. From the **yellow** section of Table 5 it can be seen that an increased viscosity of the liquid used in the slurry gives a decrease in reaction rate. Moreover, when comparing the **blue**, **green**, and **yellow** section it seems that a higher concentration of LiH gives a higher reaction rate.

Most of the liquids used exhibit a limited solubility in water, with the exception of glycerol and benzyl alcohol which are both highly soluble. The solubility of the liquid in water was expected to have an influence on the reaction rate since the liquid to

some extent separates the LiH from the water. However, the limited amount of tests performed does not indicate a relation between reaction rate and solubility.

4.1.3 DEPOSITS FROM THE REACTIONS USING SEAWATER

After repeated testing using seawater and LiH both as slurry and as pure powder some white deposits on the surface of the stainless steel reaction vessel became more and more apparent from each test. The deposits were most apparent in the area where most of the reaction is expected to have occurred. A picture of the deposits inside the end of the reaction vessel can be seen in Figure 11.

FIGURE 11: PICTURE OF DEPOSITS IN REACTION VESSEL

The end cap where the LiH was placed for each tests has been removed, as can be observed in Figure 11. This is to better show the inside of the reaction vessel where most of the deposits occurred. As mentioned, the reaction vessel was thoroughly flushed between each test with water, followed by acetone before dried using flowing air. Consequently the deposits are not likely to be very soluble in water or acetone at room temperature. The deposits were scraped off the reaction vessel using a stainless steel spatula, and were then examined under a microscope. It appeared to

be a crystalline solid, and upon contact with 3 molar sulphuric acid it reacted giving effervescence and bubbles visible in the microscope.

Please note that experiments performed using deionised water did not give any deposits. Additionally, it has not been concluded whether the deposits are related to the liquid used in the slurry or not.

4.1.4 DEPOSITS FROM THE REACTION OF POWDERED LITHIUM HYDRIDE

For comparison to the tests using LiH suspended in slurry some tests were performed using pure LiH powder. In the tests using slurry the reactant was "painted" in the end cap, and due to the wetting angle, surface tension, and viscosity of the slurry it stayed there even when the system was inverted. To mimic this behaviour the LiH powder was wrapped in tissue paper which was held in place by friction against the internal wall of the reaction vessel.

On these tests a solid white slug of a similar to double the mass of the initial reacted LiH was found contained within the paper wrapping. Regarding the mass, it is worth noting that the white solid was not properly dried before weighing. Upon contact with 5% dilute acetic acid it continued to react slowly giving off bubbles. Two of the white slugs were reacted with water and the gas bubbles were collected to determine the volume expelled. The amount of gas liberated upon complete reaction was in the area of 1-2 ml. The type of gas was not verified.

Please note that on the tests using LiH suspended as slurry however, there were no white solids to be found.

4.1.5 CONCEPTUAL MODEL AT ATMOSPHERIC PRESSURE

Based on the results presented in 4.1.1 and 4.1.2, and the procedure explained in 3.1.2 the following experiment was performed. The recorded results consist as mentioned of time of reaction and amount of expelled water per unit mass of LiH. The results can be seen in Table 6.

TABLE 6: HYDROGEN GENERATION AND REACTION RATE FOR SUITABLE SLURRIES

Amount LiH [g]	Slurry-liquid	Ratio LiH:liq	Time of reaction [s]	Volume expelled [ml]	Volume per mass LiH [ml/g]	Comments:
0.0346	Olive oil	1:30	90	110	N/A	
0.1107	Mobil DTE H/M	1:2	12	110	N/A	Incomplete fuel delivery
0.0592	Mobil DTE H/M	1:5	18	130	N/A	

The slurry compositions used in these experiments are chosen due to slow reaction rate, which consequently reduce the risk for an uncontrollable increase of internal pressure in the apparatus. Table 6 indicates that higher concentrations of LiH increase the rate of reaction. Unfortunately little can be deduced from these experiments about the amount of generated hydrogen per gram of reactant due to incomplete fuel delivery, thus rendering the results not applicable. The reason for still showing this column is that this was an important parameter the test was designed to uncover. This is a consequence of the small amounts of fuel, which in turn results in a high percentage loss due to residual fuel left on the outlet of the syringe. This is also the reason for only performing 3 test runs, as the experiment was deemed too inaccurate to give valuable quantitative results. Nevertheless, the practical problems faced here results in valuable knowledge for the design process of the intended system, and for the experiment presented in the following chapter.

4.1.6 PILOT STUDY AT ELEVATED PRESSURES

Although the results from this experiment in general have been deemed invalid, some interesting observations were made during the pilot study. One such observation was the formation of a white solid slug that would continue to slowly react with water even after being exposed to water in the reaction chamber for over 30 min under pressure. It only occurred when the pressures exceeded 100 Barg, and it repeatedly had a seemingly identical shape and size of a cylindrical depression in the end cap where the LiH powder was placed before reaction.

4.2 REACTION PARAMETERS UNDER PRESSURE

This chapter gives a comprehensive depiction of the influence of essential parameters on the reaction. It begins with an explanation on how the data has been interpreted, followed by subsequent representations to distinguish the different aspects of the reaction. These are the time of reaction, pressure increase from reaction, percentage completion, and generated buoyancy.

4.2.1 AN INTRODUCTION TO THE RESULTS

This chapter gives an introduction to the results obtained from the reaction of LiH with water and seawater at elevated pressures. It further defines the various reaction parameters that are used in chapter 4.2. Figure 12 shows the experimental results for pressure before reaction versus percent of complete reaction.
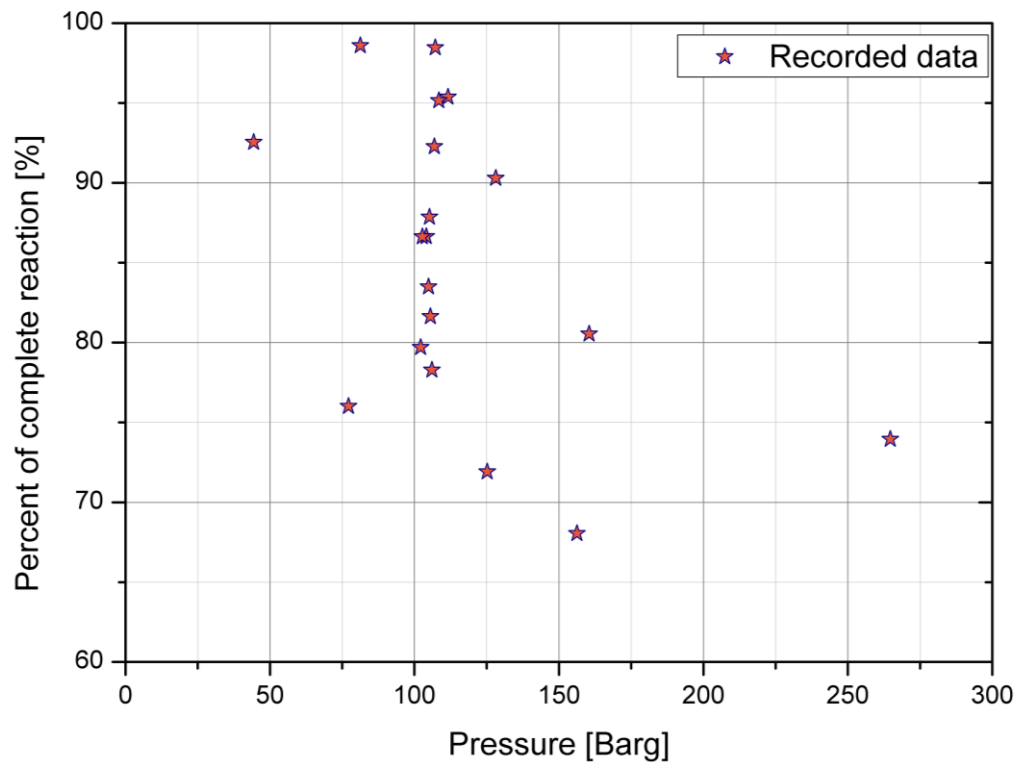
FIGURE 12: EXPERIMENTAL TEST RESULTS AS A FUCTION OF PERCENTAGE COMPLETION

One star in Figure 12 represents a single test run where the pressure is taken at initiation of reaction, and the percentage of complete reaction is based on expected pressure rise for stoichiometric amounts of hydrogen (please see chapter 3.3 and current for further details). Each test run typically lasts 1-1.5 h including preparation and clean-up. In addition to a collective comparison of the results, more detailed graphs for each run have also been recorded. The three following figures are showing the same selected test run, and the graphs are used to explain points of interest and comparison used in the work presented in this thesis. The first of these three figures is Figure 13 which shows a complete test run from the start of the pre-charging of hydrogen, to the dissolution process of hydrogen in the water along with a drop in temperature after reaction.

FIGURE 13: PRESSURE OVER TIME IN A COMPLETE TEST RUN

The blue line in Figure 13 is the pressure over time before reaction, whereas the green is during and after. Pressure at Time=0 represents the pressure of gaseous hydrogen delivered from the hydrogen supply at the point where needle valve 1 (see Figure 8 and Figure 9) has been closed. After this, the water pump is started,resulting in a rise in pressure. This is a consequence of the fact that the volume available for the gaseous hydrogen is being occupied by the introdu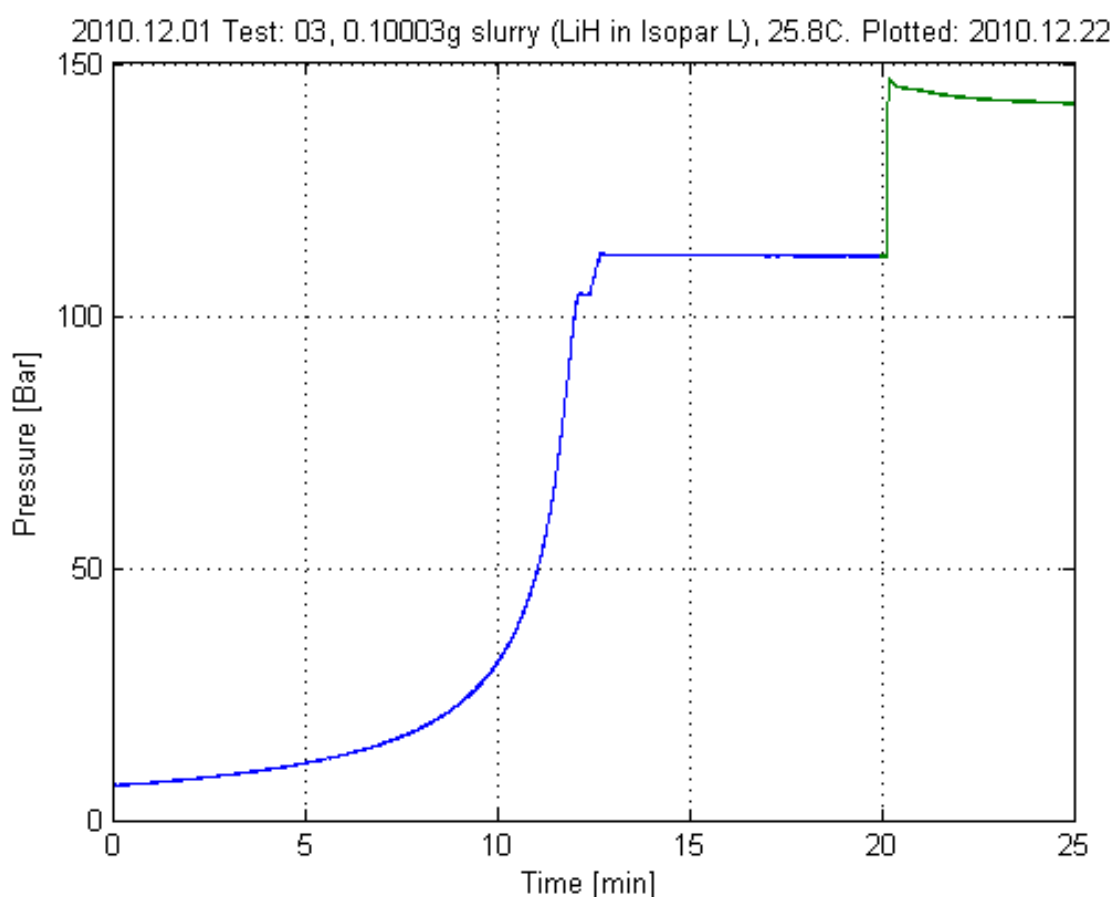ced water. Although the water delivery rate is constant the pressure rise is not, following $\Delta P = (P_1 * V_1)/\Delta V$, where state 1 is at Time=0. This however is a simplified depiction as the hydrogen will dissolve in the water as pressure rises, hydrogen is not an ideal gas, and it assumes isothermal conditions. In the end of the steep increase in pressure on the blue curve a notch can be observed before the beginning of the flat section. This notch represents stopping of the pump. The following increase in pressure is a result of the closing of needle valve 2 (see Figure 8 and Figure 9) which decreases the volume of the system. During the following flat section the system is equilibrating in terms of dissolution of hydrogen and temperature. As the system appears to be in equilibrium, the reaction is initiated, (see detailed explanation in chapter 3.2.2). This results in a rapid rise in pressure, as seen in the beginning of the green line in Figure 13. After this, a smaller, yet initially rapid, drop in pressure can be observed. The rate of pressure loss levels out and seems to converge to a constant decay, which is to be expected if the drop is caused partly by a minor leak and partly by the dissolution of hydrogen until equilibrium is reached. The cause of this drop will be discussed in more detail in chapter 5.2.1. The rapid rise in pressure is presented in more detail in Figure 14.
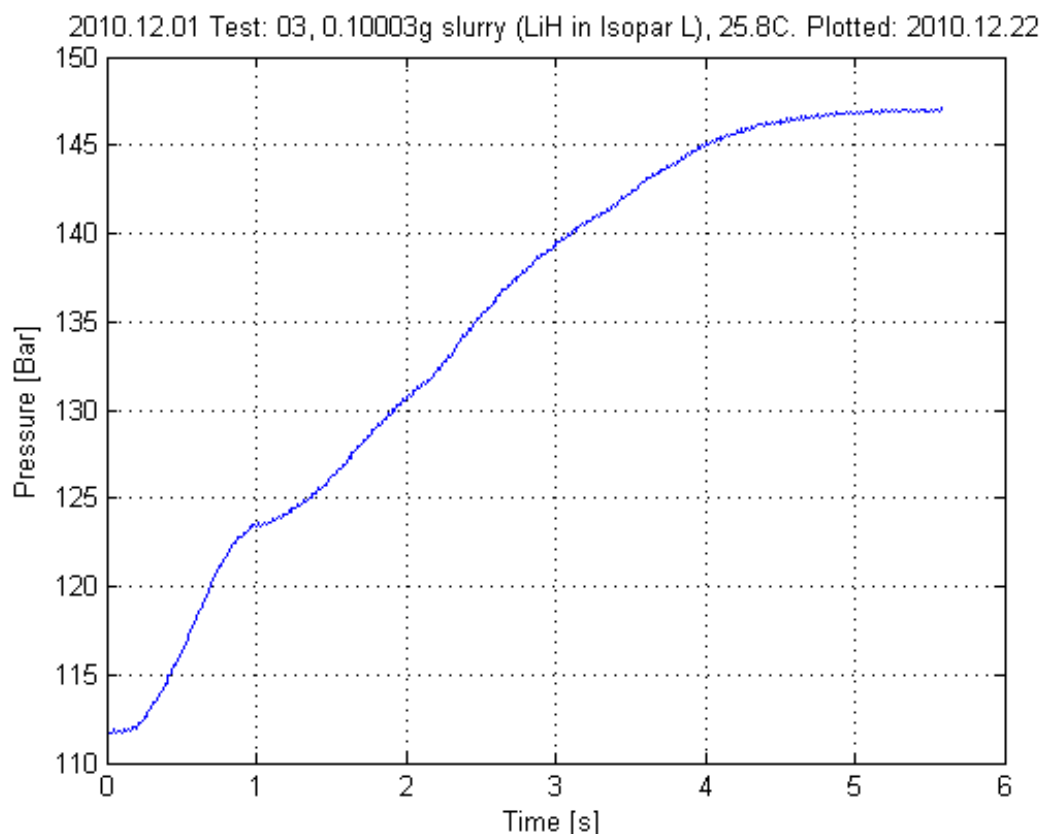
FIGURE 14: PRESSURE OVER TIME FOR AN ISOLATED REACTION

The blue line in Figure 14 shows recorded pressure over time for a section of the recorded data where t=0 is equivalent to the beginning of the rapid rise in pressure just after t=20 minutes in figure 13. This section is referred to as **the time of reaction**, and is defined as time between minimum and maximum pressure in the recorded data which is also used later in this thesis. Please note how the reaction exhibits a nearly linear rate for most of the reaction period. This is presentable for most of the tests investigated. The same recorded reaction is shown with the blue line in Figure 15 below, but here including the dissolution process and equilibration of temperature that happens after the reaction has occured.
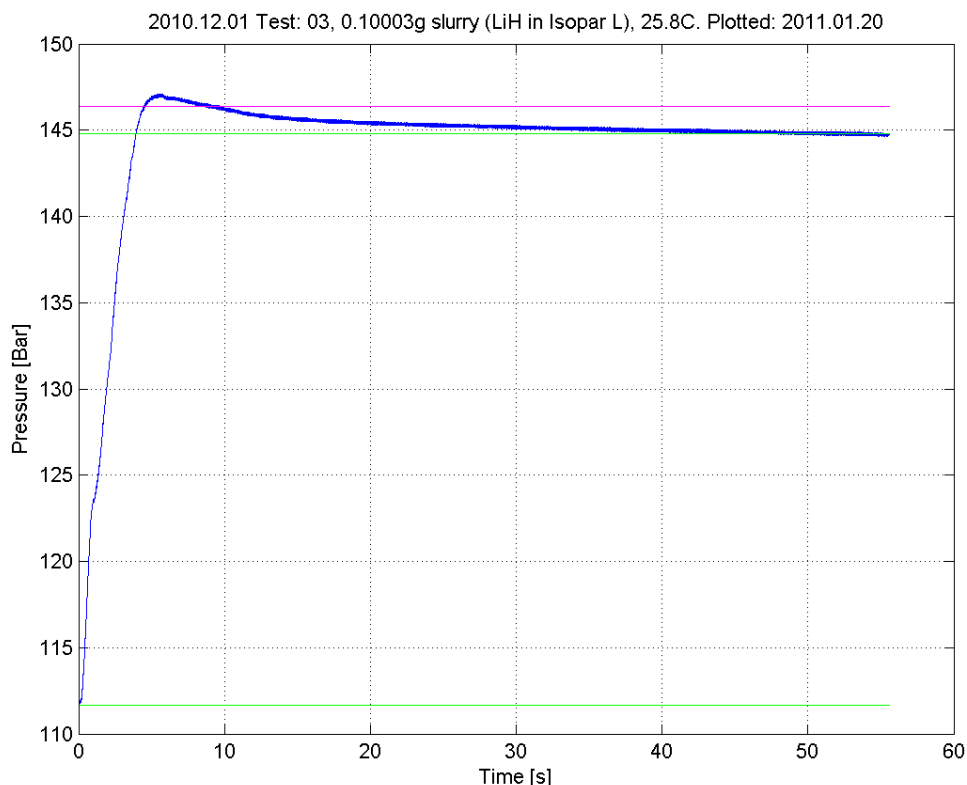
FIGURE 15: REACTION AND DISSOLUTION OF HYDROGEN COMPARED TO THEORY

The time before cut off of the reaction shown above is set to be 50 s after reaching maximum pressure, and does consequently not represent any set criteria to pressure drop rate or similar. The reason for this simplistic cut off is the many variables between different tests which may influence the dissolution process and drop in temperature. Consequently it becomes difficult to define an appropriate comparable cut off point. Some of these variables are pressure, amount of reactant, and water and slurry media. The two horizontal green lines represent the **start and end pressure of reaction**, where start and end is defined as minimum pressure and a set time after maximum pressure respectively, as previously explained. The difference between these two pressures gives **the increase in pressure with reaction**, as referred to later in this thesis. The pink horizontal line represents the expected pressure after complete stoichiometric reaction and acts as a theoretical comparison to the upper green line. This comparison is the basis of **percentage of complete reaction**, as referred to later in this thesis.

56

These results for each test run has been quantified, as explained and **marked in bold** in the current chapter. The data forms a collective dataset, as previously shown in Figure 12 where one star represents one test. The test runs shown in Figure 12 is presented in further detail in chapters 4.2.5 through 4.2.5.

4.2.2 TIME OF REACTION

The time of reaction is a product of reaction rate and amount of reactant. The reaction rate may be influenced by several factors like method of delivery of reactant, contact area between the reactants, and ambient conditions. Figure 16 shows the time of reaction at respective initial pressures as a function of amount of reactant. The legend for this figure is also used for Figure 18 and Figure 21, where a dark blue circle represents 0.025 g LiH, a red diamond represents 0.05 g LiH, and a green triangle represents 0.1 g LiH.
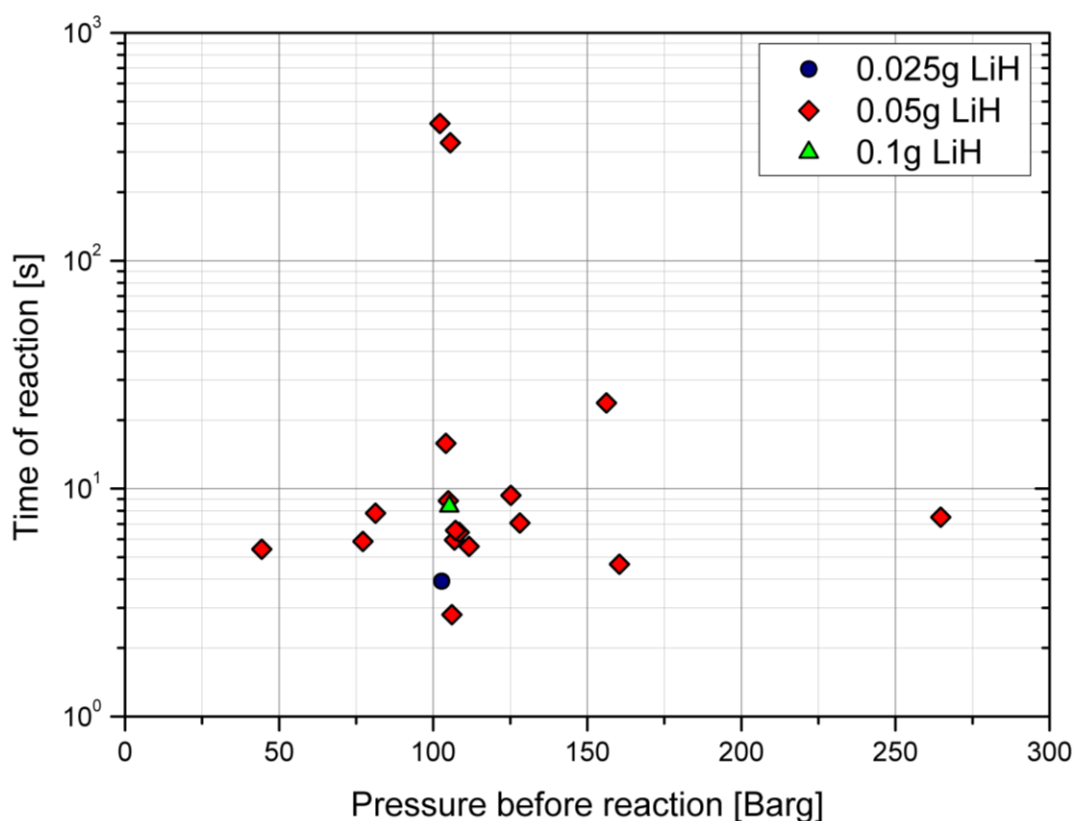
FIGURE 16: TIME OF REACTION AS A FUNCTION OF AMOUNT OF REACTANT AND INITIAL PRESSURE

57

In the tests shown, the area of contact between the reactants has been kept constant to eliminate this effect. Nevertheless, little is known of distribution and mixing of the reactants through the course of the reaction, thus there may be an influence that cannot be determined. As can be seen in Figure 16 there is a large spread in time of reaction between tests of seemingly similar parameters. Consequently, the same tests are shown in Figure 17 as a function of delivery method of the LiH, and type of water used. In the legend in Figure 17, as well as in Figure 19, the colour of the centre of each data point depicts which type of water that has been used in the test. A blue centre represents seawater, and red represents deionised water. Moreover, the geometric shape as well as the colour of the outline of each point refers to the delivery method of LiH. The same geometric shape and outline colour represents the same whether it is using deionised water or seawater. A square with a red outline represents pure LiH powder wrapped in tissue paper; further a circle with cyan outline represents LiH suspended in Isopar L oil in a 1:1 ratio by weight, or gravimetric. Similarly, a triangle with green outline represents LiH suspended in Mobil H/M (Heavy/Medium lubrication oil), also in a 1:1 gravimetric ratio.
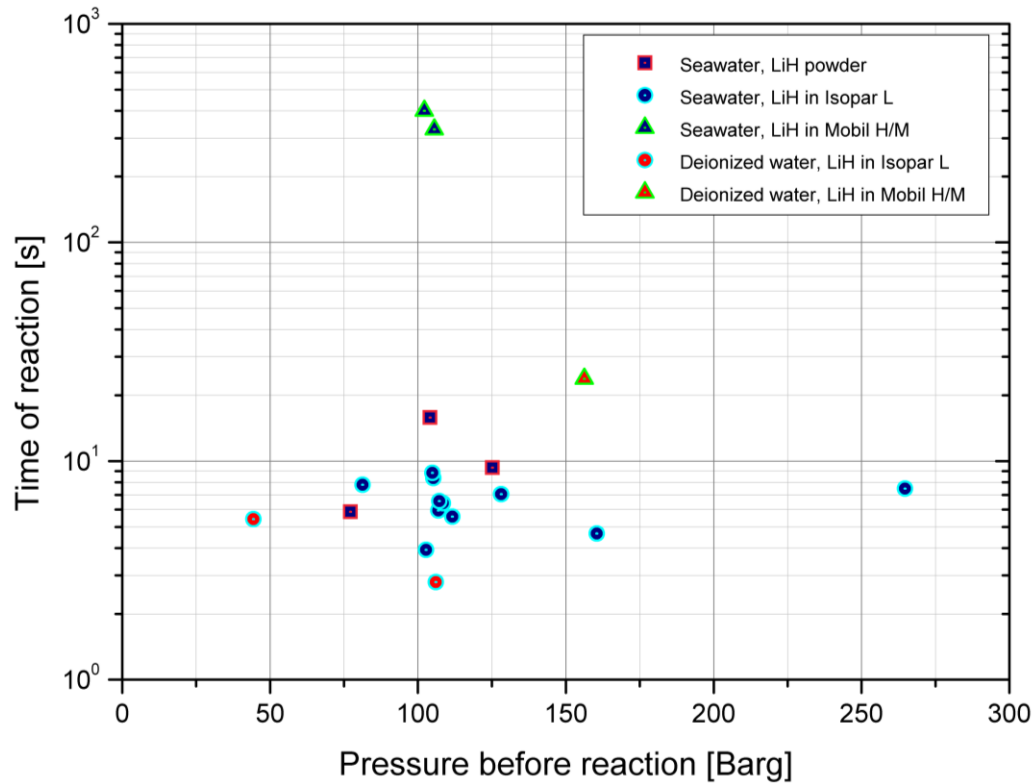
FIGURE 17: TIME OF REACTION WITH DIFFERENT TEST PARAMETERS

From Figure 17 it can be observed that the tests using LiH suspended in Mobil H/M reacted with seawater gives a significantly longer reaction time. For the same slurry used with deionised water a similar effect can be seen, although in this case it is much less apparent. An additional indicated trend is that the reaction time seems to be shorter for tests using deionised water compared to those using seawater where the remaining parameters are similar.

When comparing the two figures it can be observed that the tests using 0.025g LiH and 0.1gLiH both are suspended in Isopar L and reacted with seawater. As all tests are done with an initially similar area of contact between the reactants, the reactions with more LiH are expected to take longer to reach completion. The one test for 0.025 g show 4 s, and the one test for 0.1 g show between 8 and 9 s, whereas the five comparative test for 0.05 g range from 5 to 9 s. Consequently, the preceding figures do support a relation between amount of reactant and time of reaction, but the results are inconclusive due to the large variation and the limited number of results. Based on the tests performed with 0.05 g LiH suspended in Isopar L reacted

with seawater in a range of 80 to 270 Barg initial pressure, there are no indications that the pressure of reaction has an effect on reaction rate.

4.2.3 PRESSURE INCREASE FROM REACTION

The reaction between LiH and water is contained within a reaction vessel of constant volume. Since the reaction gives off gaseous hydrogen and the volume stays constant, the pressure will increase inside the reaction vessel. This pressure rise is shown in Figure 18 as a function of pressure before reaction and amount of LiH.
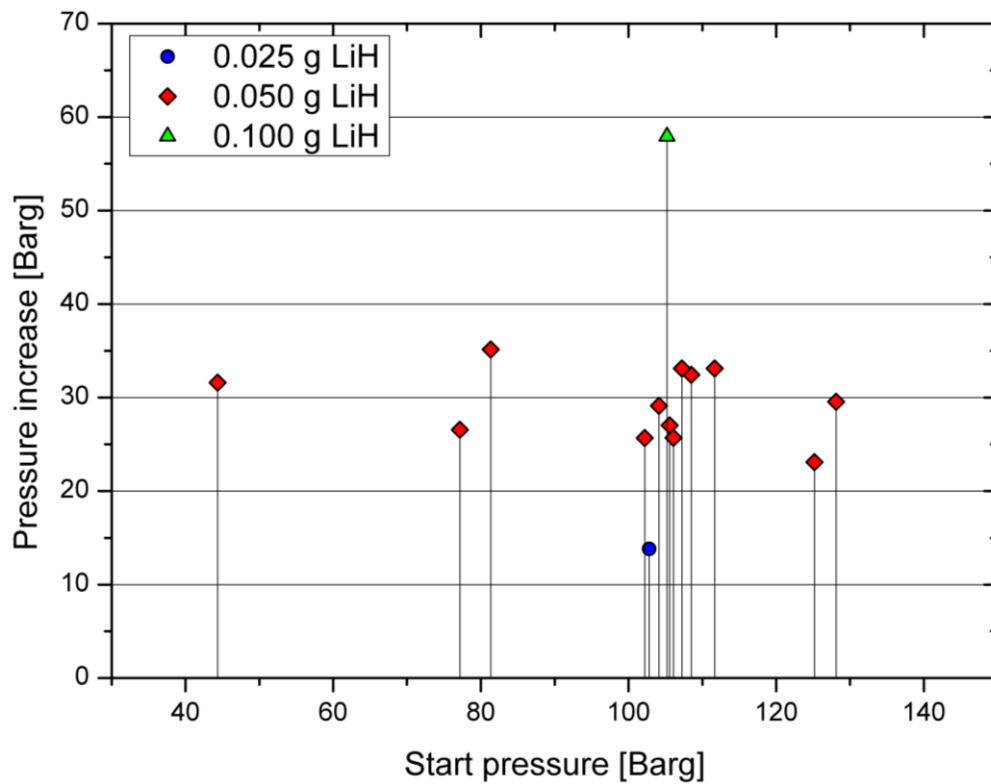
FIGURE 18: INCREASE IN PRESSURE WITH REACTION

Due to practical aspects of the experimental test setup some tests were performed at slightly differing test parameters that can and have been easily accounted for in the data processing of other output parameters. However, in the isolated parameter of pressure increase with reaction, this is not as simple. Consequently the tests presented in Figure 18 are a selection of the total amount of tests that have been

performed. The pressure before reaction and the pressure increase presented can be added together to represent the pressure after reaction.

The one test performed with 0.1 g LiH has a pressure increase close to 60 Bara. The test using 0.05 g, or half the amount of reactant, show an approximate average of 30 Bara pressure increase, which corresponds to half the pressure. Similarly, also the quarter of 0.1 g, 0.025 g, shows a quarter of the pressure increase at approximately 15 Bara. This nearly linear relation between the amount of LiH and the recorded increase in pressure with reaction follows expectations from literature. However, since only one test has been performed at 0.1 and 0.025 g respectively, these results do not prove any relation. Nevertheless, since it does follow expectations from theory, it is expected to represent physical significance. This finding will not be further discussed.

4.2.4 COMPLETION OF REACTION

The percentage completion of reaction is based on a comparison of the recorded increase in pressure, to the expected increase in pressure at the given parameters. Figure 19 shows the completion of reaction as a function of the type of delivery of reactant and the type of water.
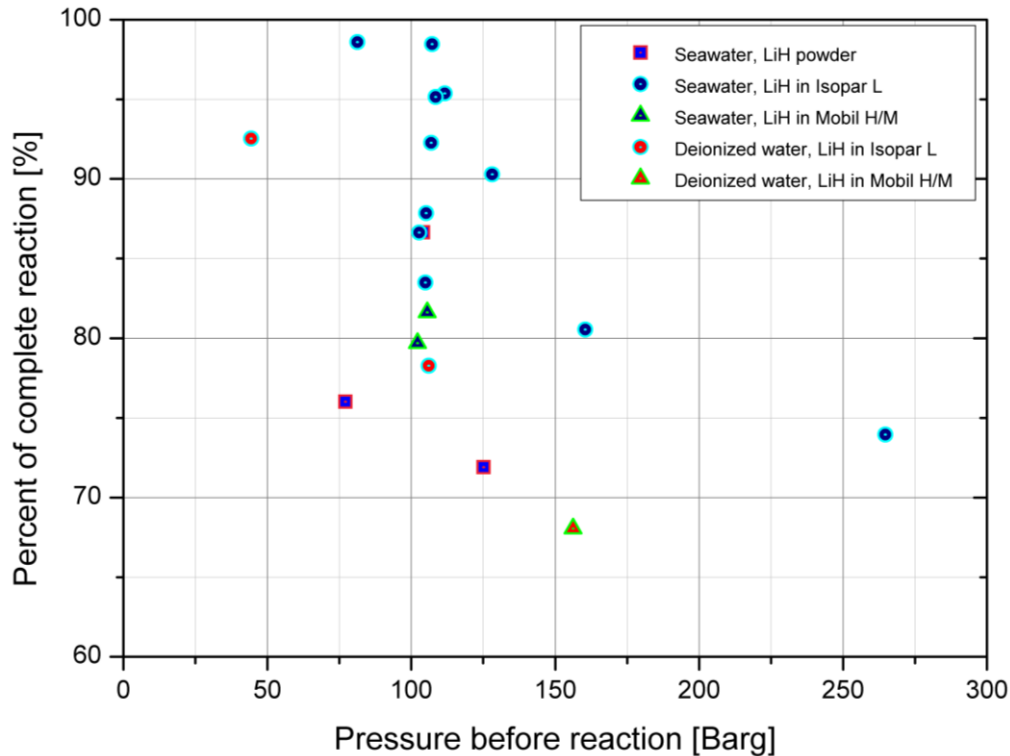
FIGURE 19: COMPLETION OF REACTION WITH DIFFERENT TEST PARAMETERS

As can be seen in the limited amount of tests shown in Figure 19, at a specific pressure, the tests using Isopar L tends to yield a higher percentage of complete reaction than the tests using LiH powder or LiH suspended in Mobil H/M. That being said, the 7 tests performed at similar conditions using seawater, LiH in Isopar L, and at approximately 110 Barg initial pressure varies from approximately 84 to 98% completion. This relatively large spread in Figure 19 calls for a presentation of seemingly identical slurries of different batches. This is shown in Figure 20 where the same colour of the centre and geometric shape has been used. Due to differentiation between two batches that both contain LiH and Isopar L in a 1:1 ratio, the outline colour has been altered from the previous figure. A red outline refers to batch number 6 of slurry, whereas a green outline refers to batch number 7. The numbers 6 and 7 does not imply anything further than the chronological order of which they have been mixed during testing
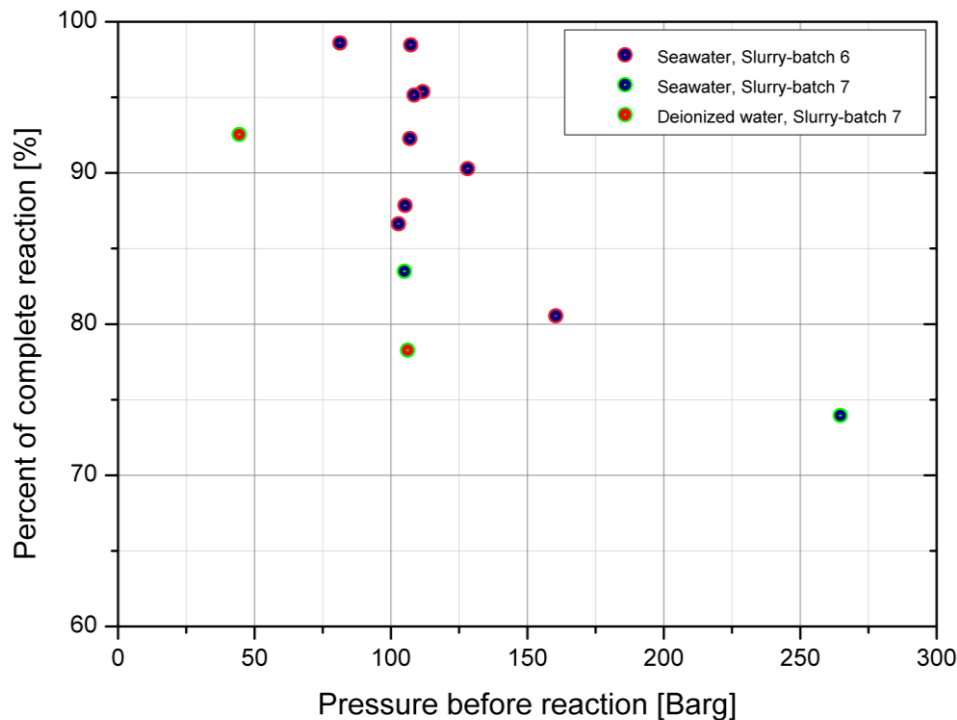
FIGURE 20: COMPLETION OF REACTION USING LITHIUM HYDRIDE IN ISOPAR L

From Figure 20 it becomes clear that not enough tests have been performed to indicate a difference between the slurries given the spread and varying test parameters.

Figure 12, Figure 19 and Figure 20 presents different aspects to the same test runs. When studying Figure 19 and Figure 20 closely, a trend of decreasing percentage of complete reaction with increasing pressure can be observed from the tests using seawater and LiH in Isopar L. Similarly in the tests using deionised water and LiH in Isopar L there are indications that this is the case also here. It is worth noting though that only two tests have been performed for this set of parameters. For the remaining parameter-sets, the spread and scarcity of the data points give no indications as to whether or not this may be a trend. Nevertheless, if there is a trend of decreasing percentage of completion with increasing pressure, then it can be observed that tests using seawater may give a higher percentage yield than the tests using deionised water. Be that as it may, if there is not a trend of decreasing yield with increasing pressures, neither is there a trend of a higher yield with seawater than deionised water to be observed.

63

4.2.5 GENERATED BUOYANCY

For the applied use in an underwater glider the amount of generated buoyancy at depth is the main determining factor for the proposed propulsion systems efficiency. Due to the compressibility of hydrogen and the solubility of hydrogen in seawater, the amount of generated buoyancy is highly dependent on pressure. Figure 21 shows the relation of buoyancy with pressure as a function of ratio of LiH to water.
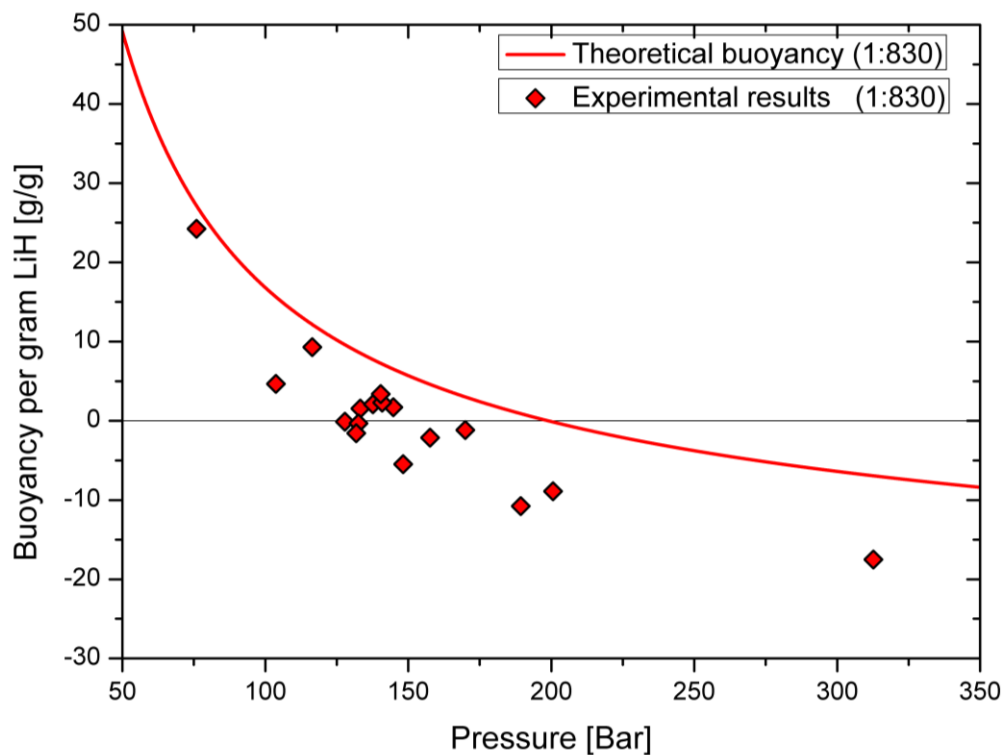
FIGURE 21: GENERATED BUOYANCY AS A FUNCTION OF PRESSURE COMPARED TO THEORETICAL MODEL

The red diamonds shown in Figure 21 represents the experimental results at the final pressure after reaction. These selected results are all using approximately 0.05g LiH reacted in approximately 41.6 ml of either deionised water or seawater giving a ratio of approximately 1:830. In addition to the test results represented by the red diamonds, also a theoretical prediction for the same concentration is presented in the thick red line. In this model, the water is assumed to be containing no hydrogen whatsoever, whereas in the experiments the water is assumed to be saturated. Consequently, the experimental results have been manipulated to exhibit

comparable results by subtracting the molar quantity of hydrogen dissolved at initial pressure in the experiment from the recorded generated molar quantity from reaction. This dissolved amount is based on theoretical predictions, as presented in chapter 2.5.3, and the assumption of saturation in experiment contra the assumption of no dissolved hydrogen in seawater. Moreover, since the solubility data is based on pure water, the subtraction is not favourable of the experimental results in terms of maximum hydrogen yield. Consequently, based on the aforementioned theory and assumptions, Figure 21 presents the least favourable and therefore most conservative interpretation of the experimental data compared to the predictive model.

Parts of the experimental data have been presented as if giving negative buoyancy. This is not actually the case, but a result of how the generation of buoyancy is defined and how the experiment has been designed. In the experiment, the water is assumed to be completely saturated with hydrogen, whereas in the ocean the water is assumed to contain no hydrogen prior to reaction. As a result, if the reaction was done in the ocean, more hydrogen could be dissolved than at comparative parameters in the experiment. Because of this, the amount of buoyancy generated has been defined as the amount of hydrogen generated in the experiment minus the amount of hydrogen that could have been dissolved in the ocean. When this subtracted amount exceeds the molar quantity generated in the experiment the result is a mathematically negative amount of hydrogen generated, thus giving negative buoyancy. In reality, this situation would simply result in zero buoyancy being generated as all the hydrogen from the reaction would dissolve in the water without reaching saturation. The reason for presenting the experimental results as negative buoyancy is to be able to show to which degree the theoretical prediction follows the experimental results, regardless of its lack of physical relevance.

Similarly to the percentage completion of reaction presented in chapter 4.2.4, also the generated buoyancy presented in Figure 21 seems to show less hydrogen generated than the theoretical model of which it is compared to. From this it may seem that less than 100% of stoichiometric reaction has occurred, but this will be further discussed in chapter 5.2. The predictive theoretical model is presented for a range of concentrations in the following chapter.

4.3 PREDICTIVE THEORETICAL MODEL

Based on the same principles as the theoretical comparison used with the experimental results in chapter 4.2, a prediction of the maximum theoretical output is presented in this chapter. The maximum yield at elevated pressures is predominantly limited by the amount of hydrogen that is dissolved in the water. Consequently, at higher concentrations of LiH to water the hydrogen will also be higher. Reference [28] reports a maximum LiH to water ratio of 1:25 to achieve complete reaction. Similarly reference [45] reports a ratio of 1:15-20. These are both at elevated pressures, yet at lower pressures than what is of interest in an underwater glider. At higher pressures this ratio may or may not differ from the two reported values, but there are little indications to be found of such a relation. Figure 22 presents the predictive theoretical model developed in relation to this thesis for a range of concentrations where the thick red line corresponds to the thick red line in Figure 21.
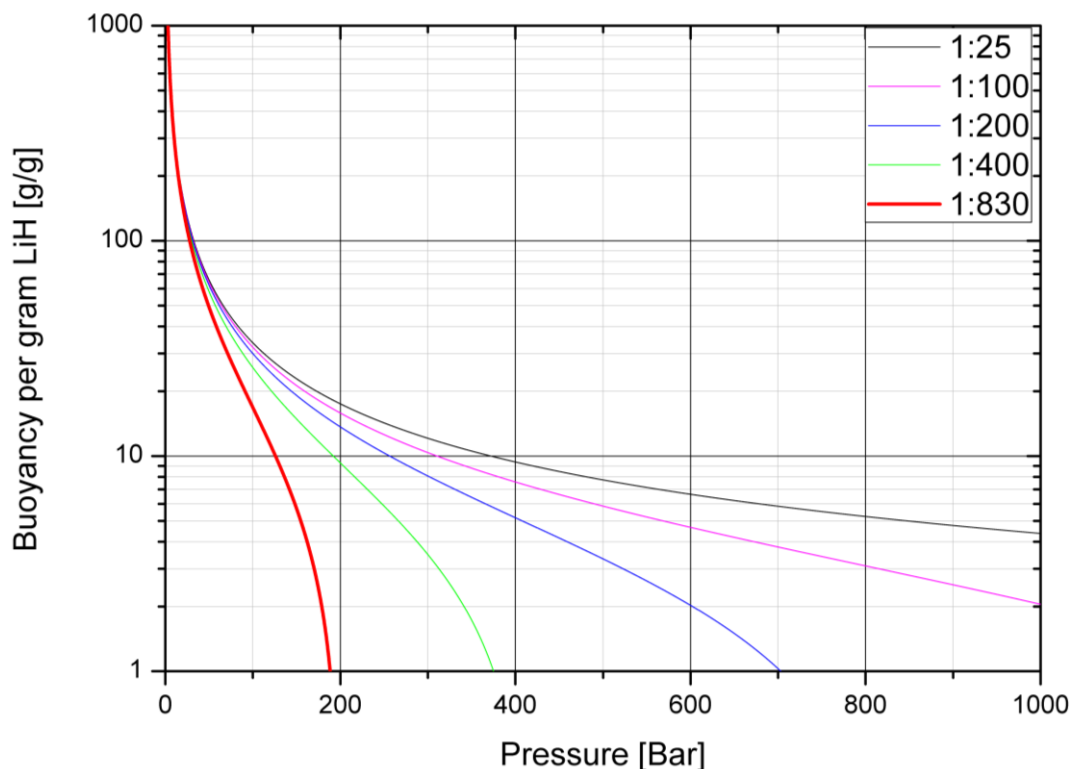
FIGURE 22: THEORETICAL GENERATION OF BUOYANCY AT A RANGE OF CONCENTRATIONS AND PRESSURES

The range of concentrations presented above span from 1:830, as tested in the work presented in this thesis, to 1:25 which as explained acts as a predicted upper limit to achieve complete reaction. On the logarithmic y-axis showing generated buoyancy as grams buoyancy per gram LiH the lower limit is set to 1. The reason for this is that a ratio of 1 g pure LiH to 1 g buoyancy can be stated to be the lower limit of interest in use in an underwater glider. Arguably, the lower limit should be set much higher for most applications. To give a more practically applied and intuitively understandable depiction of the same model, Figure 23 below includes the mass of the liquid in the slurry, showing the total mass of LiH-slurry needed to achieve 300 g of buoyancy in seawater at depth. Also here the colours of the lines correspond to the same concentrations presented in previous figures.
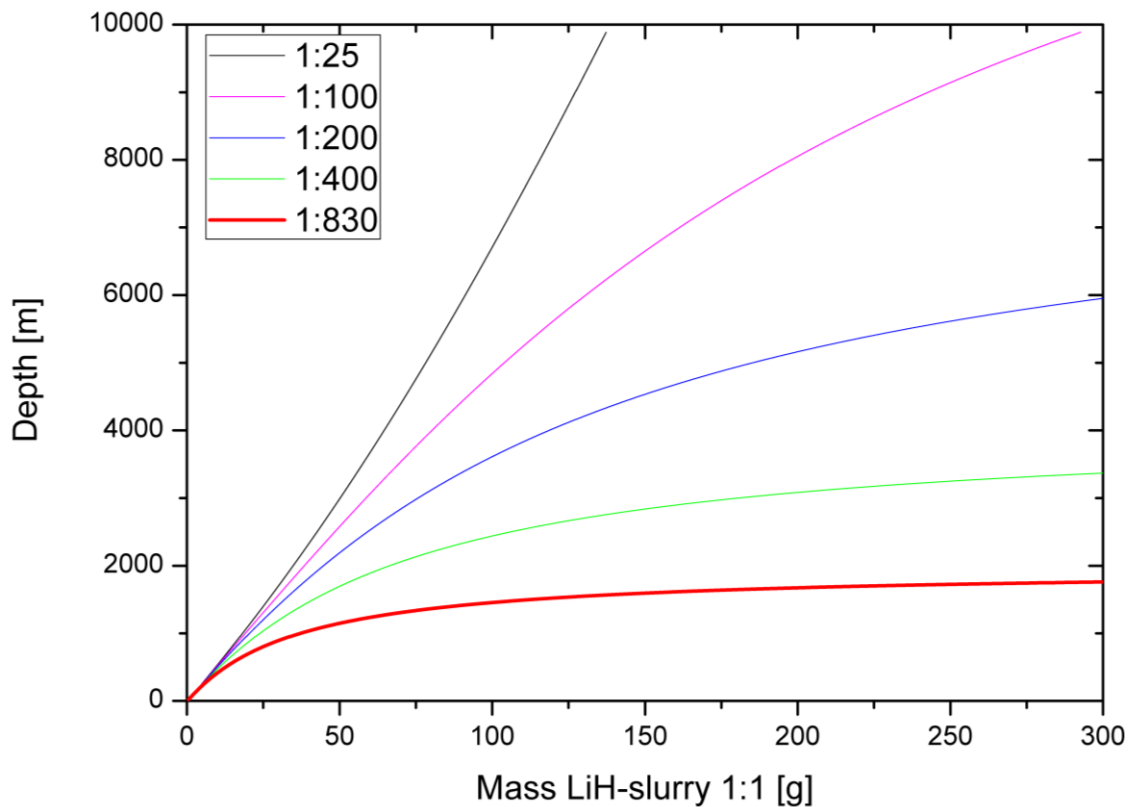
FIGURE 23: MASS OF SLURRY NEEDED FOR 300 G BUOYANCY AT DEPTH AS A FUNCTION OF CONCENTRATION

From Figure 23 it becomes clear that the amount of LiH-slurry needed to generate a given amount of buoyancy as a function of depth is highly dependent on the

concentration of LiH to water. The upper limit of the x-axis in Figure 23 is set to the point where 300 g of LiH-slurry is needed to achieve 300 g of buoyancy. This would correspond to 2 g buoyancy per gram of LiH in Figure 22. The reason for depicting the amount of slurry needed for specifically 300 g of buoyancy is discussed in chapter 5.3.

5 DISCUSSION

For the successful development of the CBD it is crucial to fully understand all the influencing factors on the chemical reaction upon which the system is based. The potential implications caused by deposits, the gains that can be made from altering the composition of the slurry, and other practical considerations are discussed within this chapter. This is followed by a discussion on how the experimental results compare to the theoretical prediction. Finally, an ideal theoretical performance is proposed and compared to the performance of the underwater glider named "Spray".

5.1 PRACTICAL CONSIDERATIONS

In the development of the proposed CBD, there are several practical challenges that must be addressed and solved before adequate functionality for autonomous operation can be achieved. This chapter discusses the practical challenges that have emerged from the work performed until this stage of development, and considers solutions where applicable.

5.1.1 CONTROL OF REACTION RATE AND TIME OF REACTION

The reaction rate must be engineered to suit the application. The performed experiments that have been presented in previous chapters have shown that the rate of reaction between LiH-slurry and water can vary greatly depending on the influencing parameters. For example, from 4.1.2 it can be deduced that for LiH suspended in slurry, the ratio of LiH to liquid has a significant influence on the rate of reaction at atmospheric pressures. Moreover, also the type of liquid has a notable effect on reaction rate which agrees with references [28, 32]. Of the material properties considered, the viscosity appears to be the element with the biggest influence; whereas, the solubility in water does not seem to have a major effect.

The reason for the viscosity to have such an effect compared to solubility is believed to be related to the range of time in which a reaction reaches completion. Of the tests performed with a gravimetric ratio of 1:2 for LiH to liquid at atmospheric pressure, all tests reached completion within 5 s. In this time span none of the liquids

69

tested would be completely dissolved at this amount and area of contact. However, as a grain of LiH comes into contact with water, gaseous hydrogen is generated, resulting in a rapid volumetric expansion. A lower viscosity liquid will experience a greater local change in shape or internal flow as a result of the same expansion since less energy can be absorbed in the liquid. As an analogy, this is much like a shock absorber which will change its dampening characteristics with changing temperatures due to the subsequent change in viscosity in the working fluid. Consequently, a lower viscosity liquid will have a greater probability of exposing another of the suspended grains of LiH to the water, so the reaction will proceed more quickly. This corresponds with the observation that the low viscosity liquids very quickly spread out on the surface of the water; whereas, this effect was not as apparent with higher viscosity liquids. Based on the same theory, it may be argued that the increase in reaction rate is not necessarily a direct result of the viscosity, but a result of the increase in contact area between the reactants. Similarly to the increased exposure of LiH due to lower viscosity and/or surface area, a greater ratio of LiH to liquid increases the probability of exposing the suspended LiH grains as the reaction proceeds. The rate of reaction can easily be controlled by altering the composition of the slurry; with reaction rates ranging from less than 1 s to well over 1 minute at atmospheric pressures, and from 2 s to over 5 min at elevated pressures. A practical consideration based on 10m accuracy of final depth of an underwater glider, a constant glide angle of 20 degrees, and a speed of 0.5 m/s, gives approximately 1 min for the reaction to reach completion. A lower limit can be argued to be in the area of 1 s, as a more rapid reaction than this may prove difficult to safely contain within a reaction vessel.

Regarding the apparent relation of variations in reaction rates with pressure, it is worth noting that the contact area of reaction was larger in the tests performed at atmospheric pressure. Yet contrary, the ratio of LiH to liquid in the tested slurries is higher in the tests performed at elevated pressures. Consequently, a direct comparison becomes difficult, thus the effect is contributed to variations in the reaction parameters. This is reinforced by Figure 16, which shows no apparent relation between pressure and time of reaction when the remaining reaction parameters are kept similar. Moreover, for reactions at different pressures and ratios of LiH to water, but with the same slurry composition and type of water, there is little

variation in time to be observed (as can be seen from Figure 17). In the example of LiH in Isopar L reacted with seawater, the reaction times range from 4-10s. Also in Figure 17, a trend of increasing reaction times with seawater compared to that of deionised water may be observed. This is believed to be due to decreasing solubility of hydrogen in water with increasing salinity [57-59]. A decrease in solubility will decrease the chemical potential and consequently influence the reaction rate, as explained in 2.5.1. Further implications of the slurry composition are discussed in the following chapter.

5.1.2 COMPOSITION OF THE SLURRY

In addition to reaction rate, the slurry composition will have an impact on other practical aspects of the proposed concept. The conceptual design presented in 2.4.5 requires neutrally buoyant slurry to function. For simplicity, the slurries used in the performed experiments consist of LiH suspended in one liquid, which results in positive buoyancy since both components have a density lower than that of water. This does not exclude the option of designing slurries of more than two components to achieve the desired properties.

For instance, the use of surfactants to improve the storability of the slurry in terms of stable suspension [32]. Similarly, a mix of a positively buoyant hydride (e.g. LiH) and a negatively buoyant hydride (e.g MgH$_2$) with a proven liquid (e.g. Isopar L) may be one way to achieve this specific property of neutral buoyancy. Alternatively, zinc or aluminium could be mixed with the LiH slurry to increase the slurry's density and possibly also generate hydrogen from a reaction between the current bi-product LiOH and the added metal. An even more exotic solution could be to explore the complex Al(BH$_4$)$_3$ which is a liquid in itself at ambient conditions [24]. In other words, there are many opportunities left to explore to achieve better practical yielding of hydrogen.

The work presented in this thesis focuses on slurries with two components, of which one has remained to be LiH. From all the liquids tested, it seems that petroleum derivatives like Isopar L and fatty oils like olive oil are of most interest, since they have not been observed to significantly react with the hydride. This may be due to the non-nucleophilic nature of LiH. That the un-reactive liquids happen to be

hydrophobic does not seem to inhibit the reaction upon exposure to liquid water, yet it may improve the long-term storability of the slurry, as it will to some extent protect the suspended LiH from humidity. The long-term storability of various slurries however has not yet been explored.

Worth noting is the degradability of olive oil and other biodegradable liquids like bio-diesel which may become important in limiting any impact on the environment surrounding the underwater glider while in operation. A practical aspect that may jeopardise functionality is deposits of bi-products of the reaction. This is considered further in the next chapter.

5.1.3 DEPOSITS FROM THE REACTIONS USING SEAWATER

Any deposited solids from the reaction of LiH with water may potentially be harmful for the proposed Chemical Buoyancy Drive, as it can prove to be detrimental to the functionality of valves, orifices, and other mechanical parts. This chapter discusses the not very soluble deposit that gradually accumulated from repeated reactions of LiH with seawater at elevated pressures.

As mentioned under 4.1.3, a thin white layer of a crystalline solid gradually built up from repeated tests, despite periodical flushing with seawater. Although no more than a fraction of 1g was deposited in total after 16 tests at said parameters, it is nonetheless a potential hazard for the continuing functionality of the buoyancy drive; especially since it is not likely to be very soluble in seawater. It did, however, react with sulphuric acid forming bubbles visible under the microscope. This, along with the limited solubility in water gives an indication that the deposited crystalline solid may be either lithium carbonate or lithium fluoride, since they are stated to exhibit limited solubility in water yet high solubility in sulphuric acid [61]. Regardless of what material the deposit is made of, it may pose a potential risk that should be thoroughly assessed and further investigated.

5.1.4 DEPOSITS FROM THE REACTION OF POWDERED LITHIUM HYDRIDE

The reaction of powdered LiH with seawater under pressure resulted in a reaction product of larger lumps of white solid. This chapter contains a discussion on the influence of the reaction parameters and the constituents of the deposits, followed by a discussion of the mechanisms of formation. These mechanisms are of interest since they may influence aspects of the reaction also at other reaction parameters.

This deposit occurred only when LiH powder wrapped in tissue paper was used. The deposit was a white solid slug of similar to double the mass of the initial LiH. The solid slug was wrapped in the paper after reaction. The paper stayed intact, with the exception of a slight change in colour, possibly due to the alkalinity of the reaction. It is consequently assumed that the paper is not a chemical contributor to the deposited slug. Similarly, the liquids used in the slurries are also believed to be largely inert and are consequently disregarded as a chemical inhibitor to the formation of said deposit. Considering the relatively large amount of deposit, it is unlikely that the salinity of the seawater is a significant contributor to the content itself; although it may still have an effect on the mechanisms of formation. This has not been further investigated through tests using powdered LiH and deionised water; consequently this deposit may not be unique for only seawater. Moreover, the mechanisms behind this formation are of interest, as they may give indications of problems that could potentially occur also with LiH suspended in slurry if the amounts or concentrations are increased.

Before the mechanisms of formation can be determined, knowing the constituents of the deposits can be helpful. Based on the preceding discussion, the two significant active constituents left are water and LiH; thus the slug is likely consisting of mostly LiOH following Equation 1 presented in 2.5.1. More accurately the reaction is in this case believed to be somewhere in between Equation 2 and Equation 3 presented in the same chapter. The fact that the slugs dissolved in both water and in dilute acetic acid further backs up this explanation. Additionally, the observed effervescence upon dissolution may indicate some remaining unreacted LiH left in the deposit, which would also explain the slightly lower volumetric hydrogen yield from these reactions,

as indicated by Figure 19 in chapter 4.2.4. The mechanisms for the formation of this LiOH deposit will now be discussed.

In the formation of the soluble LiOH deposit, the slurry liquid and the paper have been ruled out as chemical contributors; nonetheless, they do seem to make the difference between formation or not. One explanation could be that the suspension of LiH in a liquid inhibits compression of the LiH powder into a solid due to pressure. However, most of the pressure build up happens while the LiH is in contact with the hydrogen and not the water. For this reason it is not likely that there is any significant pressure differential within the powder, as the hydrogen molecules can readily pass between the dry LiH particles. Subsequently, it is also unlikely that the powder will be compressed into a solid as a result of the increasing pressure.

Another explanation could be that the paper reduces the water flow to and from the reactant through the course of the reaction, consequently maintaining a locally more concentrated LiOH solution. Reference [49] states that a higher LiOH concentration will reduce the rate of dissolution of the LiOH formed in the interface between the LiH and the water. This is due to a resulting smaller difference in chemical potential which is what drives the dissolution process. When getting closer to saturation, the reaction will almost stop [49]. Consequently, it is reasonable to believe that not only is this the mechanism causing the slug at said conditions, but with higher LiH to water ratios it may come into play also at other conditions. An alternative perspective based on a similar logic, could be that the exposure level of the LiH, and consequently the reaction rate (Equation 2), exceeds the rate of the LiOH dissolution (Equation 3). This could cause a decrease in chemical potential thus passivating the reaction by the build up of a LiOH layer.

To counter the likelihood of either of the above mentioned mechanisms taking effect, a high degree of convection or surface area compared to amount of reactant will need to be maintained. This argument is supported by the high pressure pilot study, where the reported deposit formed in a depression in the reaction vessel, consequently having a smaller area of reaction compared to amount of reactant. It can further be induced that the effect may become more apparent at larger amounts of reactant at a given concentration, because this will result in a comparatively smaller ratio of area of reaction to volume of reactant based on the geometrical

considerations of the delivered fuel (ref. area to volume ratio e.g. for a sphere with increasing radius). Alternatively, using slurry exhibiting a slower reaction rate (Equation 2) may prove preferential.

5.1.5 MISCELLANEOUS CONCEPTUAL DEVELOPMENT

This chapter briefly discusses three remaining aspects of the practical development and design to be completed before reaching satisfactory functionality of the proposed system. More improvements may be discovered at a later stage. The three covered aspects are fuel delivery, fuel storage, and use of a fuel cell for the generated hydrogen; presented in this order.

The tests presented in 3.1.2 and 4.1.5 showed some difficulties in complete and accurate fuel delivery in the tested amounts (which was less than 1 g in total per test). In the conceptual model, the fuel delivery outlet is likely to be in direct contact with water when there is to be no reaction occurring. This is not expected to be a conceptual limitation, since, for instance, hydrogen has shown to be a good separator of the two reactants, as presented in 3.2.2. Nevertheless, it needs to be taken into account in the design. Valve functionality and other moving parts in contact with the slurry are also worth thorough consideration due to the readily reactive and corrosive nature of the slurry.

Further, the long-term storage properties of slurries of different compositions needs to be investigated before the concept will be ready for repeated dive cycles.

Developing a system to use the hydrogen in a fuel cell to generate additional energy is a major project in itself. This will not be discussed further than what has been presented in 2.4.4 of the literature review, and in chapter 5.3.

5.2 COMPARING EXPERIMENTS TO THEORY

The experimental results can be portrayed through many different variables, as shown through chapter 4.2. The final and arguably most important output parameter is the amount of generated buoyancy, as this will determine the range in an underwater glider. This amount of generated buoyancy per mass of fuel is presented

in Figure 21 as a comparison to the theoretical prediction. Even though there is significant scattering to be seen, the experimental results does deviate from the theoretical prediction at the same concentration. Further there may be a trend of increasing deviation with increasing pressure. This deviation can be caused by three things, an inaccuracy in the experiment, faulty assumptions in the theoretical model, or a physically incomplete reaction.

The accuracy of the experiment has already been presented in 3.2.4. The assumptions made in the theoretical model have been presented in 3.3.1, yet the assumption of complete instantaneous dissolution of hydrogen in the water is further discussed in the following chapter. Following this is a discussion of the degree of completion of the reaction. Finally a brief conclusion is presented.

5.2.1 COMPLETION OF THE DISSOLUTION OF HYDROGEN

The theoretical prediction assumes instantaneous and complete dissolution of hydrogen, as explained in 3.3.1. From Figure 13 found in chapter 4.2 little change in pressure is observed shortly prior to the reaction, indicating that the dissolution process is close to saturation, as little more hydrogen is dissolved. After the reaction however, there is a significant pressure drop that can be more closely observed in Figure 15. As presented in 2.5.1 the reaction of LiH with water is exothermic by approximately 175 kJ/mol. Consequently, even though the temperature is expected to be constant before reaction, this is not the case after. Given that the volume of hydrogen is dependent on temperature, the observed drop could just as well indicate a change in temperature as dissolution of hydrogen.

The accurate rise in temperature in the hydrogen from reaction is difficult to determine without having a thermocouple measuring the temperature through the course of the reaction. However, it is believed to be initially higher than for the water due to the lower heat capacity of hydrogen to that of water, and the amount of time at which the reaction occurs. Consequently, the hydrogen is expected to experience a rapid rise in temperature followed by a drop, as the thermal energy is absorbed in the water and also the stainless steel reaction vessel until equilibrium. Following this a slower equilibration process is expected as the thermal energy is transferred to the

surroundings. This explanation is quite coherent with the presented reaction in Figure 13.

Since the temperature change has not been recorded it is difficult to accurately determine how much of the pressure drop that is caused by the change in temperature, and how much that is caused by dissolution. However, when studying Figure 13 it can be observed that the pressure increase from start to finish of reaction is modest compared to the total pressure increase before reaction. Additionally, the rate of pressure increase in the end of both charging and reaction is comparable. So when there is not much drop in pressure to be observed after the charge process, it cannot be expected to be a significant drop after the reaction either. Consequently, the drop that can be observed after reaction is largely contributed to the drop in temperature

5.2.2 COMPLETION OF THE REACTION BETWEEN LIH AND (SEA)WATER

The percentage completion of the reaction between LiH and water or seawater is a comparison of the experimental results to the same theoretical model as presented in Figure 21. Therefore, it is used herein to explain the deviation of generated buoyancy between the experimental results and the theoretical prediction. Figure 19, Figure 20, and Figure 21 exhibit a similar deviation, thus incomplete reaction is a likely explanation.

From the same figures, a trend of decreasing yield with increasing pressure may be observed. This however is difficult to say for sure, as the scattering of the results are of a similar size as the deviation from theory, and the amount of results are limited. Furthermore, since no work has been published for the tested conditions, there are no solid indications in the studied literature that this should be expected. Consequently, this indicated trend cannot be given much significance.

An indicated trend from Figure 19 and Figure 20 is a higher percentage yield of hydrogen with seawater than with deionised water. Also here the results are scattered, but this phenomenon is expected. This is because the theoretical model calculates the expected hydrogen yield based on the solubility of hydrogen in deionised water for both deionised water and seawater, despite the fact that the

solubility decreases with increasing salinity [57-59]. Consequently, since it follows theoretical expectations, the results are considered to depict a physical relation between hydrogen yield and salinity. A quantified relation however cannot be derived from the test results.

Figure 19 show that Isopar L gives a higher percentage yield of hydrogen than Mobil H/M and pure LiH powder. As previously mentioned in 5.1.3 under "Soluble deposits", there seems to be LiH left after reaction in the tests using pure LiH. Whether some LiH is left after reaction also in the tests using Mobil H/M has been difficult to determine. The performed tests do not show why the slurry has an influence on the percentage completion. Nevertheless, there are strong indications that the composition of the slurry has an influence on the reaction, which indicates that the percentage yield may be improved.

5.2.3 SUMMARY

The accuracy of the experiment cannot be completely ruled out as a possible explanation for the deviation between experimental results and theoretical expectations. Nevertheless, there are other factors that have been accounted for, and the conclusions are presented below.

It is concluded that there is a physical lack of completion of reaction. Further it is indicated that this percentage of completion can be improved with slurry composition. A relation between pressure and completion is indicated, but the results are inconclusive. Finally, the assumption of complete dissolution before and after reaction may be slightly misleading, although it is not likely to account for much of the offset from the predicted buoyancy generation.

Consequently, with the exception of the given assumptions and the accuracy of the results of which is it based upon, the theoretical prediction is regarded as correct.

5.3 THEORETICAL PREDICTION OF PERFORMANCE

The predicted buoyancy has been compared to theoretical results at a concentration of LiH to water by mass of 1:830, and the validity of this comparison was discussed in detail in the preceding chapter. At higher concentrations of LiH, the hydrogen yield is expected to increase. However, at some concentration, the reaction is expected to cease. The concentration at which this is expected to occur is roughly 1:25 and has been discussed in chapter 4.3. The reason for this has not been thoroughly discussed in the referenced literature [28, 45]. However, as indicated in [49], one explanation could be that the reaction stops due to the concentration of the reaction product LiOH in the water reaching saturation. The solubility of LiOH in water is 12.5 g for every 100 g of water at 25°C [61]. Given a molecular weight of 23.95 g/mol for LiOH and 7.95 g/mol for LiH, this relates to a gravimetric ratio of 1:24 of LiH to water. Consequently, it is likely that this is the explanation for a ceased reaction depending on ratio. That being said, the given numbers are for atmospheric pressures; whereas, the pressure of interest will be significantly higher. The solubility of a solid in a liquid is dependent on pressure, but since the volume of solution decreases with the addition of LiOH as presented in 2.5.4, it is likely that this effect works in favour of the reaction rather than against it. Unfortunately, no research has been found that presents this relation for the given conditions.

Considering Figure 23 in chapter 4.2.5 for the concentration of 1:25, a mass of 26.7 g of slurry is needed to achieve 300 g of buoyancy at 1500 m depth. This is based on complete reaction, a 1:1 gravimetric ratio of LiH to inert liquid in the slurry, a constant density for seawater of 1030 g/l and solubility for hydrogen in deionised water. The slurry has been regarded as neutrally buoyant, despite the fact that the tested slurry has been positively buoyant. It is worth noting that seawater does compress with pressure resulting in a higher density, and exhibits a lower solubility of hydrogen than deionised water. Counteracting this, the solubility of LiOH is believed to be lower for seawater than for deionised water. Consequently, these three factors have been disregarded for simplicity due to a shortage in the studied literature.

The buoyancy of 300 g at 1500 m depth mentioned above are parameters chosen specifically to be comparable to the performance of the commercial underwater

glider Spray, as presented in [1]. For this comparison, however, it is worth noting that the slurry used is positively buoyant, whereas the batteries in Spray are negatively buoyant. This, along with the need to isolate the batteries from the outside pressure by the use of a pressure vessel, makes an accurate comparison difficult. However, as an assumption, a 1:1 gravimetric ratio of battery to pressure vessel and buoyancy has been used. This comparison results in 24 g for Spray contra 26.7 g from this work which translates to approximately 90% comparable efficiency. It is worth mentioning that the range of Spray at 7,000 km greatly exceeds the range of both Seaglider and Slocum Battery at 4,600 and 500 km respectively [1]. In other words, the comparative range for an underwater glider propelled by a CBD is expected to be somewhere in between that of Seaglider and Spray, depending on hydrodynamic efficiency. The related subject of electric energy for the control system is discussed in the paragraph below.

The batteries in Spray do not only power the propulsion, but also the control system and scientific payload. Consequently, to compare the predicted performance in this work to the performance of Spray, the proposed concept of using the generated hydrogen in a fuel cell for electric energy must be considered. Using a calculation presented in [62], assuming 60% efficiency of a PEMFC, we find that from the approximate 3.36 g of hydrogen, 286 kJ of electric energy are available per cycle in addition to propulsion. This compares positively to the total amount in Spray of 13 kJ per cycle; giving more than 20 times the amount of available electric energy. This increased amount of available electric energy may accommodate additional functionality in an underwater glider or other underwater vehicle. That being said, this is not an accurate depiction, as the weight of the fuel cell and oxygen storage must be included. Consequently this comparison is not to be regarded as any more than indicative.

When sending a vehicle with sophisticated scientific equipment on a mission to deep oceans, a factor of safety for its return will need to be included. At this stage in development the performance of the reaction between LiH and seawater is not known with great certainty, therefore determining a recommended factor of safety has not been attempted. The results presented here are consequently a direct depiction of the expected performance based on the predictive theoretical model, as presented in Figure 23. Since the acceptable ratio of fuel to buoyancy may vary with

the specific vehicle and mission objectives, a range of ratios are presented. For a ratio of fuel to buoyancy by mass of 1:10, the maximum depth that may be reached is 1700 m. For a ratio of 1:5 however, a depth of 3600 m is within reach. Finally, if a ratio of 1:2 is acceptable, the concept predicts operation possible to depths exceeding 10 000 m. These numbers are based on the maximum theoretical yield and consequently only act as a guideline.

6   CONCLUSION

This thesis has introduced a novel propulsion system for underwater gliders, and indicated how it compares to the existing systems. Based on the discussed results it is concluded what parts of the concept that works well, and what parts that should be improved. This chapter covers the applied use of the reaction between LiH slurry and seawater, and the subsequent challenges that are to be expected. This is followed by proposed improvements for both the CBD, and for the experimental setup that determines its performance. Finally, the predicted performance is presented.

6.1   APPLIED USE OF LITHIUM HYDRIDE SLURRY

The results presented in this thesis have shown that the reaction rate is easily controlled and that the range of reaction times is suitable for the use in an underwater glider. More work can and should be carried out to improve the current slurry, and to more accurately determine how it will work in practice in an underwater glider. However, no conceptual flaws have been discovered, and the current performance may be further improved.

The deposits that gradually build up after repeated reactions with seawater may prove to be a challenge in the development of the CBD. However, there are no indications that this will become a conceptual limitation, as it occurs in small amounts and has already been proven to be easily removed using sulphuric acid. Nevertheless, this needs to be further investigated, and a practically feasible solution to the problem needs to be developed and tested.

The deposit resulting from the reaction of powdered LiH with seawater is concluded to consist mostly of undissolved LiOH. The deposit is currently not a problem, as it does not occur while using LiH suspended in slurry. Nevertheless, it has been indicated that it may become a problem at higher concentrations of LiH in water, or at greater amounts of reactant. Consequently, this should be further investigated.

Storing and delivering the LiH fuel suspended in slurry has proven to be practically feasible. Moreover it may seem to be a preferable option compared to using pure LiH, since it seemingly eliminates the formation of said LiOH deposit. Additionally, neutral buoyancy of the fuel should be practically obtainable. Consequently, LiH slurry is concluded to be a promising concept worth further investigation.

6.2 IMPROVEMENTS OF CONCEPT

The proposed CBD is clearly a promising concept, yet there is still work to be done to improve, and more accurately verify, its functionality. The results on whether the completion of the chemical reaction between LiH and seawater is dependent on pressure are inconclusive. That being said, if there is a dependence of completion with pressure, it is not a conceptual limitation, but a minor decrease in its performance compared to the presented ideal theoretical maximum. Further it is indicated that improvements can be made through the composition of the LiH slurry.

Regarding the practical realisation of the CBD, there is more work to be done also here. Fuel delivery and storage may prove to be challenging, but there are currently no indications that these challenges will be practically impossible to solve.

The proposed concept of using a fuel cell to harvest electric energy from the generated hydrogen remains a promising future concept. Development of this system has not been attempted in the work presented in this thesis; therefore no recommendations in this regard have been presented. Nevertheless, development and implementation of such a system is encouraged.

6.3 IMPROVEMENTS OF EXPERIMENT

Despite extensive efforts of calibration, verifying sources of error, and improving the accuracy of the high pressure experiment, there are still a few things that could be improved. Firstly, the internal volume of the reaction vessel should be measured to

an accuracy of +/- 0.1 ml or better. Further, data for solubility of hydrogen in seawater at elevated pressures, solubility of LiOH in seawater at elevated pressures, compressibility of seawater, and hydrogen content at depth in the oceans should be determined and implemented in the predictive and comparative model. Finally, the temperature should be recorded; although this might prove to be difficult due to the high pressure and subsequent challenging sealing of the vessel. Additionally, the rate of reaction and the expected temperature differentials between the constituents in the reaction may also prove challenging when measuring the temperature. If these three parts of the experiment are improved, the results will likely depict the process with adequate accuracy to apply them in the propulsion of an underwater glider.

6.4 PERFORMANCE

The theoretical prediction presented herein is concluded to be valid in concept. Whether the predicted performance is achievable will need to be determined by further experiments, yet it is regarded to give a good indication at this stage.

The indicative comparison to the commercial underwater glider Spray shows 90% comparable efficiency in propulsion, and over 20 times more available electric energy.

For repeated dives in an underwater glider as it is used today, a practical maximum depth around 2000 m is proposed. However, it is indicated that operational depths exceeding 10 000 m may be possible.

Sea trials need to be performed to give indisputable proof of the concept and to obtain valuable practical experience.

7   RECOMMENDATIONS FOR FUTURE WORK

Based on the conclusions drawn from the work presented in this thesis, three recommendations have been made for the continuing development of the CBD. These recommendations are presented below:

➢ Improve the experimental setup, as covered in chapter 6.3, and continue experimental testing. Use seawater and LiH slurry at a gravimetric ratio of 1:25 of LiH to seawater, and a final pressure of 400 Barg. The results from these tests will determine the accuracy of the presented predictive model for operational depths exceeding the proposed 2000 m, and give indications to deeper operation. Continuing observation of deposits is recommended.

➢ Test a range of slurries for both reaction characteristics and storability. Both components and ratios should be adjusted with the goal of achieving low degradation in storage and a controlled delivery of the slurry. The reaction rate must be stable, and lie between 1 and 60 s. Finally, the hydrogen yield per unit mass of slurry is the determining parameter, and neutral buoyancy is required.

➢ Design and build a functional model based on the conceptual sketches presented herein, and perform sea trials. Gradual progression is advised in terms of operational depth and mission complexity. The amount of fuel should be calculated using a factor of safety of 2 or more.

8 REFERENCES

1. Rudnick, D.L., et al., *Underwater gliders for ocean research.* Marine Technology Society Journal, 2004. **38**(1): p. 48-59.
2. Davis, R.E., C.C. Eriksen, and C.P. Jones, eds. *Autonomous Buoyancy-driven Underwater Gliders*. The Technology and Applications of Autonomous Underwater Vehicles, ed. G. Griffiths. 2001, Taylor and Francis: London.
3. Stommel, H., *Direct measurements of sub-surface currents.* Deep Sea Research (1953), 1955. **2**(4): p. 284-285.
4. Swallow, J.C., *A neutral-buoyancy float for measuring deep currents.* Deep Sea Research (1953), 1955. **3**(1): p. 74-81.
5. Davis, R.E., J.T. Sherman, and J. Dufour, *Profiling ALACEs and other advances in autonomous subsurface floats.* Journal of atmospheric and oceanic technology, 2001. **18**: p. 982-993.
6. Davis, R.E., et al., *The Autonomous Lagrangian Circulation Explorer (ALACE).* Journal of atmospheric and oceanic technology, 1992. **9**(3): p. 264-285.
7. Simonetti, P., *Slocum glider: Design and 1991 field trials.* 1992, Webb Research Corp.
8. Donaldson, P., *Tracing a eureka moment.* Unmanned Vehicles, 2007: p. 17.
9. Graver, J.G., R. Bachmayer, and N.E. Leonard. *Underwater glider model parameter identification*. in *Proc. 13th Int. Symp. on Unmanned Untethered Submersible Technology (UUST)*. 2003.
10. Stommel, H., *The Slocum mission.* Oceanography, 1989.
11. Webb, D.C., P.J. Simonetti, and C.P. Jones, *Slocum: An underwater glider propelled by environmental energy.* IEEE Journal of Oceanic Engineering, 2001. **26**(4): p. 447-452.
12. Roemmich, D., et al., *Autonomous profiling floats: Workhorse for broad-scale ocean observations.* Marine Technology Society Journal, 2004. **38**(1).
13. Guizzo, E., *Defense Contractors Snap Up Submersible Robot Gliders [Update].* Spectrum, IEEE, 2008. **45**(9): p. 11-12.
14. Eriksen, C.C., et al., *Seaglider: A long-range autonomous underwater vehicle for oceanographic research.* IEEE Journal of Oceanic Engineering, 2001. **26**(4).
15. Sherman, J., et al., *The autonomous underwater glider "Spray".* IEEE Journal of Oceanic Engineering, 2001. **26**(4): p. 437-446.
16. Wang, S., et al., *Harvesting of PEM fuel cell heat energy for a thermal engine in an underwater glider.* Journal of Power Sources, 2007. **169**: p. 338–346.
17. Wood, S., *The Development of an Autonomous Underwater Powered Glider for Deep-Sea Biological, Chemical and Physical Oceanography.* 2007.
18. Alvarez, A., et al., *Fòlaga: A low-cost autonomous underwater vehicle combining glider and AUV capabilities.* Ocean Engineering, 2009. **36**(1): p. 24-38.
19. Graver, J.G., *Underwater gliders: Dynamics, control and design*, in *Mechanical and aerospace engineering*. 2005, Princeton university. p. 273.
20. Guo, C. and N. Kato, *Mini Underwater Glider (MUG) for Education*.
21. Eriksen, C.C., *Autonomous Underwater Gliders*. 2003.
22. Psoma, A. and G. Sattler, *Fuel cell systems for submarines: from the first idea to serial production.* Journal of Power Sources, 2002. **106**(1-2): p. 381-383.
23. Barbir, F., *Proton exchange membrane fuel cell technology status and applicability for propulsion of autonomous underwater vehicles*. 2002, Proton Energy Systems.
24. Orimo, S.-i., et al., *Complex hydrides for hydrogen storage.* Chemical Reviews, 2007. **107**(10): p. 4111-4132.
25. Kong, V.C.Y., et al., *Development of hydrogen storage for fuel cell generators II: utilization of calcium hydride and lithium hydride.* International Journal of Hydrogen Energy, 2003. **28**(2): p. 205-214.

26. Kojima, Y., et al., *Compressed hydrogen generation using chemical hydride.* Journal of Power Sources, 2004. **135**: p. 36-41.
27. Kong, V.C.Y., et al., *Development of hydrogen storage for fuel cell generators. I: Hydrogen generation using hydrolysis hydrides.* International Journal of Hydrogen Energy, 1999. **24**: p. 665-675.
28. DeVries, G., *High-pressure gas from Lithium Hydride and sea water*. 1965, Bureau of Naval Weapons.
29. Breault, R.W., C. Larson, and J. Rolfe, *Hydrogen for a PEM fuel cell vehicle using a chemical-hydride slurry*, Thermo Power Corporation. p. 952-956.
30. Mao, W.L. and H.-k. Mao, *Hydrogen storage in molecular compounds*, in *Proceedings of the National Academy of Sciences (PNAS)*. 2004, The National Academy of Sciences p. 708-710.
31. Züttel, A., *Hydrogen storage methods.* Naturwissenschaften, 2004. **91**: p. 157-172.
32. McClaine, A.W., et al., *Hydrogen transmission/storage with metal hydride-organic slurry and advanced chemical hydride/hydrogen for PEMFC vehicles*, in *Proceedings of the 2000 U.S. DOE Hydrogen Program Review*. 2000, Department Of E nergy Hydrogen Program.
33. Schlapbach, L. and A. Züttel, *Hydrogen-storage materials for mobile applications.* Nature, 2001. **414**: p. 353-358.
34. Ashby, E.C. and S.A. Noding, *Hydrometalation. 6. Evaluation of lithium hydride as a reducing agent and hydrometalation agent.* The Journal of Organic Chemistry, 1980. **45**(6): p. 1041-1044.
35. McClaine, A.W., S. Tullmann, and K. Brown, *Chemical hydride slurry for hydrogen production and storage.* 2004, Department Of Energy Hydrogen Program.
36. Fort, Y., *Lithium hydride containing complex reducing agent: A new and simple activation of commercial lithium hydride.* Tetrahedron Letters, 1995. **36**(34): p. 6051-6054.
37. Jeppson, D.W., et al., *Lithium literature review: Lithium's properties and interactions*. 1978, Hanford Engineering Development Laboratory.
38. Matsunaga, T., et al., *Magnesium borohydride: A new hydrogen storage material.* Renewable Energy, 2008. **33**(2): p. 193-196.
39. Huot, J., G. Liang, and R. Schulz, *Magnesium-based nanocomposites chemical hydrides.* Journal of Alloys and Compounds, 2003. **353**.
40. Christie, T. and B. Brathwaite, *Mineral commodity report 19 - Beryllium, Gallium, Lithium, Magnesium, Uranium and Zirconium*, Institute of Geological and Nuclear Sciences Ltd.
41. Li, Z.P., et al., *Protide compounds in hydrogen storage systems.* Journal of Alloys and Compounds, 2003. **356-357**: p. 469-474.
42. McClaine, A.W. and K. Brown, *Storing and transporting energy*. 2007: United States.
43. Messer, C.E., *A survey report on Lithium Hydride.* 1960, United States Atomic Energy Commision.
44. Gibb, T.R.P. and C.E. Messer, *A survey report on Lithium Hydride.* 1954, United States Atomic Energy Commission.
45. Pitcher, G.K. and G.J. Kavarnos, *A test assembly for hydrogen production by the hydrolysis of solid lithium hydride.* Int. J. Hydrogen Energy, 1997. **22**(6): p. 575-579.
46. Aral, H. and A. Vecchio-Sadus, *Toxicity of lithium to humans and the environment—A literature review.* Ecotoxicology and Environmental Safety, 2008. **70**: p. 349-356.
47. Kjølholt, J., et al., *The elements in the second rank - an environmental problem now or in the future?* 2003, Danish Environmental Protection Agency, Danish Ministry of Environment.
48. Speight, J.G., *Lange's handbook of chemistry*. Sixteenth ed: The McGraw-Hill Companies.
49. Leckey, J.H., L.E. Nulf, and J.R. Kirkpatrick, *Reaction of Lithium Hydride with Water.* Langmuir, 1996. **12**(26): p. 6361-6367.

50. Ott, J.B., J.R. Goates, and H.T.H. Jr., *Comparisons of equations of state in effectively describing PVT relations.* Journal of Chemical Education, 1971. **48**(8): p. 515-517.
51. Mortimer, R.G., ed. *Physical Chemistry*. 3rd ed. 2008, Elsevier Academic Press.
52. Kemp, M.K., R.E. Thompson, and D.J. Zigrang, *Equations of state with two constants.* Journal of Chemical Education, 1975. **52**(12): p. 802-null.
53. Leachman, J.W., et al., *Fundamental equations of state for parahydrogen, normal hydrogen, and orthohydrogen.* Journal of Physical and Chemical Reference Data, 2009. **38**(3): p. 721-748.
54. Leachman, J.W., et al., *Fundamental equations of state for parahydrogen, normal hydrogen, and orthohydrogen*, in *NIST Chemistry WebBook, NIST Standard Reference Database Number 69*, P.J. Linstrom and W.G. Mallard, Editors. 2009, National Institute of Standards and Technology: Gaithersburg MD.
55. Spycher, N.F. and M.H. Reed, *Fugacity coefficients of H2, CO2, CH4, H2O and of H2O- CO2-CH4 mixtures: A virial equation treatment for moderate pressures and temperatures applicable to calculations of hydrothermal boiling.* Geochimica et Cosmochimica Acta, 1988. **52**(3): p. 739-749.
56. Wiebe, R. and V.L. Gaddy, *The Solubility of Hydrogen in Water at 0, 50, 75 and 100' from 25 to 1000 Atmospheres.* Journal of the American Chemical Society, 1934.
57. Crozier, T.E. and S. Yamamoto, *Solubility of hydrogen in water, seawater, and NaCl solutions.* Journal of Chemical and Engineering Data, 1974. **19**(3): p. 242-244.
58. Elliot, A.J., M.P. Chenier, and D.C. Ouellette, *Solubilities of hydrogen and oxygen in concentrated lithium salt solutions.* Fusion Engineering and Design, 1990. **13**(1): p. 29-31.
59. Gordon, L.I., Y. Cohen, and D.R. Standley, *The solubility of molecular hydrogen in seawater.* Deep-Sea Research, 1977. **24**: p. 937-941.
60. Herrington, T.M., A.D. Pethybrldge, and M.O. Roffey, *Densities of aqueous lithium, sodium, and potassium hydroxides from 25 to 75 C at 1 atm.* J. Chem. Eng. Data, 1986. **31**: p. 31-34.
61. *CRC Handbook of Chemistry and Physics.* 83 ed, ed. D.R. Lide. 2002: CRC Press.
62. Borchsenius, J. and S. Pinder. *Underwater glider propulsion using chemical hydrides.* in *OCEANS 2010 IEEE - Sydney.*

APPENDIX

The appendices can be found on the attached compact disk where the contents are sorted by the following structure:

A. THEORETICAL MATLAB MODEL

B. ADDITIONAL RESULTS

    1 LEAK TESTS

    2 VOLUME DETERMINATION

C. EXPERIMENTAL PROCEDURES

D. EQUIPMENT

    1 EQUIPMENT LIST

    2 SPECIFICATION SHEETS

    3 PURCHASE ORDERS

E. RESEARCH PROPOSAL

F. PUBLISHED WORK

G. ELECTRONIC COPY OF THESIS AND LIBRARY